PhD Thesis

Boundary Condition Analysis in Topological Weyl Semimetals

Xi Wu [1]

Osaka University Particle Physics Theory Group

August 2018

[1] wuxi@het.phys.sci.osaka-u.ac.jp

Abstract

In this thesis, I take a particle theory approach for studying topological related Weyl semimetals, especially for the study of energy dispersion relations and of edge states: based on basic assumptions such as symmetry, topology, and dimension, write down Lagrangian; solve equation of motion and boundary conditions; get energy dispersion relations; and give explanation to relation between physical quantities. I call it boundary condition analysis. Fruitful results come out: the bulk and edge states are shown to be determined by conserved momenta and boundary condition parameters, new exotic states localized at the intersection of boundaries are predicted, and dispersions determined.

Acknowledgements

I give thanks my supervisor Professor Koji Hashimoto for introducing this field of research and guiding me in the process of research, publication and etc. I also thank Professor Onogi and Professor Yamaguchi for having discussions, pointing out lots of loopholes in the thesis, answering me lots of questions. I learned a lot from them. Moreover, I benefit a lot from Professor Koshino's suggestions from condensed matter physics' viewpoint and Professor Oda's suggestions in the thesis and presentation. I learned a lot about lattice model and received lots of help during collaboration from Dr. Kimura to whom I owe many thanks, too.

Contents

Chapter 1

Introduction

1.1 Backgrounds: Weyl fermions in condensed matter physics

In 1929, Professor Hermann Weyl [1] proposed his theory to describe solutions of the massless Dirac equation in which fermions are separated into two independent representations of Lorentz group and called left/right-handed or chiral fermions. Later they have been called Weyl fermions. Weyl fermion became a very important concept in particle physics after the discovery of violation of parity in weak process. It successfully describes neutrinos to be left-handed and antineutrinos to be right-handed and it was verified in pion decay [2]. Since then it became a fundamental building block for theory of weak interaction in the standard model.

In condensed matter systems Weyl fermions are realized as quasiparticles with definite energy dispersions. Instead of observing the cross-sections as in high energy experiments, condensed matter physicists start to observe the energy spectra in a crystal. Weyl fermions in crystal are discovered through theoretical prediction [3][4][5][6] followed by experimental verification [7][8][9]. It is possible that two-band Hamiltonians in three dimensions to own band-crossing points where Weyl fermions can emerge. When the band-crossing point are exactly at Fermi level, we get semimetal. This can be assured by some symmetries. As far as the band-crossing points are separated, they are topologically protected/conserved as a monopole charge. That is how it got the name topological Weyl semimetal. In Ref. [3], time-reversal symmetry is used to place band-crossing points and do the separation and Weyl semimetals are predicted to exist in between three dimensional topological insulator phase and normal insulator phase. In Ref. [4], the team of X. Wan predicted Weyl semimetal in a material — pyrochlore iridates (such as $Y_2Ir_2O_7$), and it is the inversion symmetry that did the job[1]. In Ref. [7][8] the energy dispersion of Weyl semimetal bulk states and Fermi-arc edge states are detected in material tantalum arsenide (TaAs), which respect time-reversal symmetry, by photoemission spectroscopy. In Ref. [9] the spin-orbit coupling is shown to be a

[1]If both time-reversal and inversion are present, the Kramers degeneracy makes the crossing points into a four-band degeneracy and a mass term is not avoidable, see Ref. [3].

parameter that can tune the distance of two Weyl points, also by photoemission spectroscopy.

In Weyl semimetals, the concept of handedness or chirality still plays an important role. However, the physical picture has been dramatically changed[2]: the spin degrees of freedom is replace by energy band structure so the handedness is no longer related with helicity and, instead it is reinterpreted as monopole charge in the Brillouin zone; because of periodicity of the lattice, Weyl fermion never appear alone but always in pairs with both chirality [10][11]; with a spacial boundary, there is a boundary-localized state protected by the chirality — Fermi arc, connecting left-handed and right-handed Weyl fermions in the Brillouin zone [4][6][7]. As a result, the research focus about Weyl fermions has been changed.

Fermi arcs can be regarded as an outcome from the another type of interplay between particle physics and condensed matter physics: relations between fermions in different dimensions where one is formulated on the boundary of another. These have been developed almost simultaneously in particle physics and in condensed matter physics, for instance domain wall formulation of 3+1 D massless chiral fermions in 4+1 D massive bulk fermion theory [12][13] and the gapless edge states in various kinds of gapped bulk topological phases [14][15]. In both cases, the topological number of bulk fermions protect boundary states. The boundary-localized states or edge states are regarded as a key feature of topological phases since it can be used diagnose different topological phases. Fermi arcs/edge states gives Weyl semimetal version of bulk-edge correspondence since their existence is due to bulk monopole charge. Two (spacial) dimensional topological insulators and Weyl semimetals are interconnected with each other, by dimensional reduction [4]. As a result, we can glimpse one from another. However, what is unique in Fermi arcs is that it connects Weyl cones of both chirality due to the doubling of fermions.

As we have seen above, at such an age of communications between particle physics and condensed matter physics, old ideas in relativistic quantum theories obtain new meanings. What is more, an good point of condensed matter systems is the freedom to realize all kinds of terms in the Lagrangian as an effective description in the real material, so this allows us to check our theory in the experiment, which helps us understand our theoretical tools in particle physics much better than before. This is the feedback to particle physics.

1.2 Motivation, questions and methodology

Usually, edge states are realized as a solution where the bulk Hamiltonian has sign change of mass term in/out of the material [16]. This can be regarded as a specific boundary condition. We inevitably wonder that maybe the edge state solution is due to the construction of boundary condition. We know from classical electromagnetism that from the surface of a metal, the electromagnetic field exponentially decay into the metal, which can be regarded as an edge solution, but this obviously is not generic and depend on the metallic boundary condition, for instance it should have finite conductivity[3]. However, the bulk-edge correspon-

[2]Chiral anomaly, transport properties, etc are also very important in Weyl semimetals, however, they are not directly related with the discuss of the rest part of this thesis, so I will not explain them here.

[3]See Sect. 8.1 in [17].

dence states that edge states are protected by bulk topological number, so they should exist regardless of boundary conditions. The works about edge states in the literature certainly not show this aspect clearly. Moreover, how the Fermi arc edge states behave under the change of boundary conditions is also not well studied in the literature[4]. As a resolution, this thesis attempts to understand the relation between bulk topological number and edge states through the study of generic boundary conditions.

After realizing the close and simple relation among boundary conditions, topological number and edge states, we believe that similar things may happen in more complicated situations, when we go from two-band Hamiltonian to four-band Hamiltonians. Inspired by the work in lattice gauge theory [20] in which regularized chiral gauge field theories of 3+1 dimension are realized at intersection of two boundaries which are 4+1 dimensions of 5+1 dimensional bulk spacetime, we wondered whether similar relations among states in three different dimensions can happen in topological material, more specifically whether a new exotic state can exist at the intersection of two boundaries in some topological phases as well. The general existence of such exotic state is based on a generalized argument of bulk-edge correspondence: edge state of 4D topological insulators have topological number, too [21], so it can also protect some states localized at the boundary of this edge. This bulk-edge-edge-of-edge correspondence becomes the second question that this thesis try understanding.

To study fermionoic states in condensed matter physics, the most obvious observable is the energy dispersion since it contains the most basic quantum numbers of a state — energy and momenta. In this thesis, I take a particle physics theory approach for studying topological Weyl semimetals, especially for the study of boundary conditions and energy dispersion relations of edge states: based on basic assumption such as symmetry, topology and dimension, write down Lagrangian, solve equation of motion, get energy dispersion relations and give explanation to relation between physical quantities. I show that this method can be used to study phenomena on the spacial boundary such as edge states and so on. I call it boundary condition analysis, which make things clear by analyzing, as oppose to synthesis, which constructs results by components.

1.3 The content and organization of the thesis

I will start from reviewing the facts of band topology in chapter 2, showing that some gapped and gapless band structure are topologically distinctive and that the study of band topology can be simplified from generic band Hamiltonians to Hamiltonians of free fermions in the low energy limit. This is the foundation for the validity and generality of simple Lagrangian formalism approach.

After that, in chapter 3, I will write down the continuum version of two-band Lagrangian plus a generic surface term and derive equation of motion and boundary condition. By analyzing these two equations we can get information of bulk states, edge states and boundary condition parameters: The bulk and edge states are complete determined by conserved momenta and one boundary condition parameter. Then with tight-biding lattice model, I

[4]For generic boundary conditions in topological insulators see [18][19].

will show that the boundary conditions obtained in the continuum theory appear as a low energy effective description and that all the results from the lattice model are parallel with the ones from continuum theory so that our continuum argument is valid. In the last section, I will give the interpretation of bulk-edge correspondence from the viewpoint of boundary condition parameters. Thus the boundary condition analysis on topological phases is formed.

In chapter 4, I will go to four band-systems to study more delicate structure of boundaries, including intersections of boundaries. The prediction of edge-of-edge states is the result from the boundary condition analysis. Basic methodology is the same as in chapter 3. The Hamiltonian considered plus generic boundary conditions are still completed solved. We will see that the boundary parameters give more mixed rotations between momenta. Based on the argument of bulk-edge correspondence and the result that edge states can also possess topological number, there is a guess that at the intersection of boundaries there may exist localized states, which is named as edge-of-edge states. And this is verified in the later sections of chapter 4 with the dispersion relation solved and the existence condition fixed by boundary condition parameters and momenta. Since the results become very clear, an experimental realizable model is introduced.

In the last chapter I will give a summary of the thesis with some discussions and future direction of this approach.

Chapter 2

Topological facts in energy bands

In this chapter, I am going to review the fact that energy bands can have topological structure and see that relativistic free fermions can be used as representative of topology. Moreover, topological phases support exotic states localized on the boundary — the edge states. The discussion will be started from chiral fermions appearing at band-crossing points. The global topological structure in Brillouin zone give constraints on low energy effective descriptions of electrons in crystal. The chiral fermions on the lattice are constraint by the Nielsen-Ninomiya theorem[10][11], which states that in odd dimensions on the lattice, chiral fermions always come in pair, with both chirality. In this section, I will explain how chiral fermions appear at band-crossing points, give a simple proof of the Nielsen-Ninomiya theorem and show the relation with edge states/Fermi arcs, which is called the bulk-edge correspondence. The discussion is a review of [22].

2.1 Weyl fermions exist at band-crossing points

First let's take a look at the band-crossing points. A generic two-band Hamiltonian, since it's Hermitian, can be parametrized by four real parameters as:

$$\mathcal{H} = a\mathbb{1}_2 + b_i\sigma_i\,,\ i = 1, 2, 3\,, \tag{2.1}$$

where the parameters can be functions of momenta, etc. Then the energy eigenvalues are:

$$\epsilon_\pm = a \pm \sqrt{b_i^2}\,. \tag{2.2}$$

So we can see that a describes the overall energy while b_is describe the splitting of energy and when all b_is are equal to zero two bands cross each other. When we are only interested in the behavior between two bands namely transition between them, we can define a new Hamiltonian with a subtracted:

$$\mathcal{H}' = b_i\sigma_i\,, \tag{2.3}$$

which has the form of a Weyl fermion/chiral fermion except that these b_is are not momenta and σ_is are not related with spin degrees of freedom. Yet we can still talk something about the topological property.

We can make a imitation with the chiral fermions. In relativistic quantum field theory, chiral fermions/Weyl fermions in 3+1 dimensions, which is in the chiral eigenstate of Dirac fermions, are in the irreducible representations of Lorentz group, parametrized by three momenta. Two fermions with opposite chirality are orthogonal to each other. Let's review this fact. In 3+1 dimension, massless fermions are generically describe by massless Dirac equation:

$$i\gamma^\mu \partial_\mu \psi = 0\,,\ \mu = 0,1,2,3\,, \tag{2.4}$$

where γ^μs are 4×4 matrices satisfying $\{\gamma^\mu,\gamma^\nu\} = 2\eta^{\mu\nu}$. The corresponding Schrodinger equation is

$$i\partial_0\psi = H\psi = \gamma^0\gamma^i(-i\partial_i)\psi\,. \tag{2.5}$$

This Hamiltonian commutes with the chiral operator $\gamma_5 = i\gamma^0\gamma^1\gamma^2\gamma^3$. Since $\gamma_5^2 = 1$, it has two eigenvalues ± 1. As a result, Hamiltonian matrix can be decomposed into two block forms whose eigenstate have $\gamma_5 = \pm 1$. Meanwhile, since

$$\{\gamma^0\gamma^i,\gamma^0\gamma^j\} = 2\delta^{ij}\otimes \mathbb{1}_2 = \{\sigma^i,\sigma^j\}\otimes\mathbb{1}_2\,, \tag{2.6}$$

and

$$[\gamma^0\gamma^i,\gamma^0\gamma^j] = 2\epsilon^{ijk}\gamma^0\gamma^k\gamma_5\,, \tag{2.7}$$

[1]we can use σ^is to expand the Hamiltonian:

$$H = \pm p_i\sigma_i\,, \tag{2.8}$$

Now we get two types of chiral fermions, each in an irreducible representation of Lorentz group. They can not be deformed into each other except through flip of signs of the p_is. In this sense, we can say that the Hamiltonian 2.3 is chiral in parameter space of b_i. However, this is not the end of the story. b_is are functions of p_is. Let's see the topological structure in the momentum space.

Near the crossing point p_*, we can expand b_i

$$b_i(p_j) = \frac{\partial b_i}{\partial p_j}(p-p_*)_j + \mathcal{O}(p_i^2)\,, \tag{2.9}$$

and the Hamiltonian to the lowest order is written as

$$\mathcal{H}'|_{p=p_*} = \sigma_i b_{ij}\delta p_j\,,\ b_{ij} = \left.\frac{\partial b_i}{\partial p_j}\right|_{p=p_*}\,,\ \delta p_j = (p-p_*)_j\,. \tag{2.10}$$

[1] $\gamma^0\gamma^i\gamma^0\gamma^j = -\gamma^i\gamma^j = i\gamma^0\gamma^k\epsilon^{ijk}\gamma_5 + \delta^{ij}$

This Hamiltonian basically is the same as (2.8), with p_i replaced by $b_{ij}p_j$. It has the chirality determined by the sign of determinant of b_{ij}:

$$\text{sign } \det(b_{ij})\,. \tag{2.11}$$

We can see that the chirality defined in this way is stable against any change of parameter nearby the crossing point and it's only related with the way how b_i is wrapped on sphere on p_i.

2.2 Brillouin zone constraints on Weyl fermions

The discussion in the previous subsection does not involve the periodicity of the Brillouin zone. In this subsection I will discuss the outcome of this periodicity: chiral fermions always come in pair, with both chirality. Let's prove this theorem in three steps:

(1) Assign to each band-crossing point p_α an integer – winding number.

(2) Show that this winding number is the chirality.

(3) Prove that the sum of all winding number is zero and thus the chirality is even.

First step: To consider band-crossing points, we only need to use Hamiltonian (2.3):

$$\mathcal{H}' = \overrightarrow{b}\cdot\overrightarrow{\sigma}\,. \tag{2.12}$$

At the crossing points p_α of two bands we have

$$b_i^2(p_\alpha) = 0\,. \tag{2.13}$$

For a small sphere S_α around p_α, we can define a vector field $\overrightarrow{n}$ as a normal vector field of another sphere $S_{\overrightarrow{n}}$ in the coordinate system of b_i:

$$\overrightarrow{n} = \frac{\overrightarrow{b}}{|\overrightarrow{b}|}. \tag{2.14}$$

The mapping $S_\alpha \to S_{\overrightarrow{n}}$ defines a unique winding number and the formula is given by

$$\omega(S_\alpha) = \frac{1}{8\pi}\int_{S_\alpha} d^2p\ \epsilon^{\mu\nu}\overrightarrow{n}\cdot\partial_\mu\overrightarrow{n}\times\partial_\nu\overrightarrow{n}\,. \tag{2.15}$$

Second step: From the previous discussion we see that the winding number for a given Hamiltonian is unique. Now let's calculate the winding number of Hamiltonian (2.8). Define

$$\overrightarrow{n}_\pm = \pm\frac{\overrightarrow{p}}{p}\,, \tag{2.16}$$

the winding number is

$$\begin{aligned}\omega(S_\alpha) &= \pm\frac{1}{8\pi}\int_{S_\alpha=\partial M_\alpha} d^2p\ \epsilon^{\mu\nu}\epsilon^{abc}\frac{p_a}{p}\partial_\mu\frac{p_b}{p}\partial_\nu\frac{p_c}{p}\\ &= \pm\frac{1}{8\pi}\int_{M_\alpha} d^3p\ \partial_\lambda(\epsilon^{\lambda\mu\nu}\epsilon^{abc}\frac{p_a}{p}\partial_\mu\frac{p_b}{p}\partial_\nu\frac{p_c}{p})\,.\end{aligned} \tag{2.17}$$

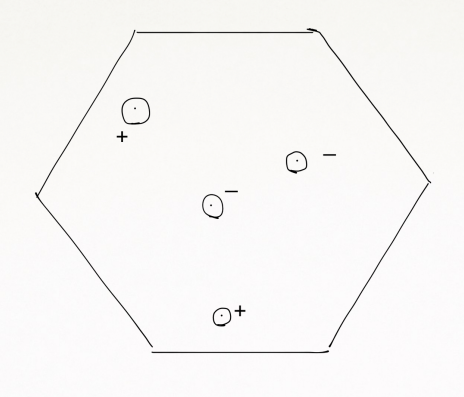

Figure 2.1: Band-crossing points in Brillouin zone

The integrant is zero except in the origin of M_α. Using

$$\partial_\mu \frac{p_b}{p} = \frac{\delta_{\mu b}}{p} - \frac{p_\mu p_b}{p^3}\,, \tag{2.18}$$

(2.17) becomes

$$\omega(S_\alpha) = \pm\frac{1}{8\pi}\int_{M_\alpha} d^3p\ \partial_\lambda(\epsilon^{\lambda bc}\epsilon^{abc}\frac{p_a}{p^3}) = \pm 1\,. \tag{2.19}$$

As a result. the winding number ± 1 corresponds to $\pm$ chirality.

Third step: Since the Brillouin zone is periodic, the boundary is only at the singular points, so that the sum of the winding numbers can be written as integrations in the Brillouin zone.

$$\begin{aligned}\sum_\alpha \omega(S_\alpha) &= \sum_\alpha \frac{1}{4\pi}\int_{S_\alpha} d^2p\ \epsilon^{\mu\nu}\overrightarrow{n}\cdot\partial_\mu\overrightarrow{n}\times\partial_\nu\overrightarrow{n} \\ &= \sum_\alpha \frac{1}{4\pi}\int_{\mathcal{B}} d^3p\ \partial_\lambda(\epsilon^{\lambda\mu\nu}\overrightarrow{n}\cdot\partial_\mu\overrightarrow{n}\times\partial_\nu\overrightarrow{n}) \\ &= \sum_\alpha \frac{1}{4\pi}\int_{\mathcal{B}} d^3p\ \epsilon^{\lambda\mu\nu}\partial_\lambda\overrightarrow{n}\cdot\partial_\mu\overrightarrow{n}\times\partial_\nu\overrightarrow{n}\,,\end{aligned} \tag{2.20}$$

But $\partial_\lambda\overrightarrow{n}$s are tangent vectors of the small sphere S_α, so $\epsilon^{\lambda\mu\nu}\partial_\lambda\overrightarrow{n}\cdot\partial_\mu\overrightarrow{n}\times\partial_\nu\overrightarrow{n}$ is zero. As a result,

$$\sum_\alpha \omega(S_\alpha) = 0\,. \tag{2.21}$$

2.3 States localized on the boundary – edge states

In this subsection, I will talk about the outcome of the band-crossing points and the Nielsen-Ninomiya theorem. At the boundary of a material, we can solve the Schrodinger equation with appropriate boundary condition. In addition to plane wave solution permeates the bulk, we can also get boundary-localized solution. Let's do it for a simple Weyl fermion with Hamiltonian:

$$H = -i\sigma_i \frac{\partial}{\partial x^i} \,. \tag{2.22}$$

An appropriate boundary condition is such that it keeps the Hamiltonian Hermitian:

$$\langle \mathcal{H}\psi_1 | \psi_2 \rangle = \langle \psi_1 | \mathcal{H}\psi_2 \rangle \,. \tag{2.23}$$

If boundary is chosen to be $x^1 = 0$,

$$(\sigma_2 - 1)\psi|_{x^1=0} = 0 \tag{2.24}$$

is an appropriate boundary condition. Now the momentum p_1 is not conserved at the

Figure 2.2: Fermi arc

boundary, but p_2 and p_3 are still good quantum number. To get an boundary-localized edge states, let's set

$$\psi \propto \exp(-\alpha x^1) \,, \tag{2.25}$$

with some real number α and solve the Hamiltonian eigen equation with the boundary condition

$$\begin{cases} (i\alpha\sigma_1 + p_2\sigma_2 + p_3\sigma_3)\psi = \epsilon\psi \\ (\sigma_2 + 1)\psi|_{x^1=0} = 0 \,. \end{cases} \tag{2.26}$$

The result is

$$\alpha = p_2 \,, \epsilon = p_3 \,, \tag{2.27}$$

and the edge state obtained is

$$\psi = \exp(-p_2 x^1 + i p_2 x^2 + i p_3 x^3)\psi(p)\,, \tag{2.28}$$

in which the normalization factor is put into $\psi(p)$.

Next let's discuss the effects of the Nielsen-Ninomiya theorem on the edge state. In the low energy $\epsilon = 0$ limit, p_3 goes to zero, so the dispersion of the edge state becomes a one dimensional line parametrized by p_2 . From (2.28), the edge state is only normalizable when $p_2 > 0$, and at $p_2 = 0$ it becomes indistinguishable from a plane wave – bulk state. In a lattice model, there are two ends of this curve corresponding to opposite chiral fermions bulk states. This comes from the requirement of periodicity of the momenta. Consider the subspace of Brillouin zone supporting edge states, the boundaries of the subspace are at band-crossing points. Because of the periodicity, the sum of the winding number of the crossing point has to be zero. As a result, the two ending point have to have opposite chirality. In general, at the boundary momentum space parametrized by p_2 and p_3, the energy ϵ depends both on p_2 and p_3 and also the boundary condition. In such a case, consider the space spanned by p_2, p_3, ϵ, In the low energy $\epsilon = 0$ limit, there is some constraint on p_2, p_3. As a result, the dispersion still becomes a one dimensional curve connecting two opposite chiral bulk states. In Sec. 3.4 in the next chapter, I will show the explicit derivation and figures of edge states and bulk states.

Chapter 3

Analysis in 3D Weyl semimetals

As discussed in previous sections, in the continuum limit in 3+1D, two-band systems with finite numbers of band touching points can be described by Weyl fermions In this chapter, I will show the how to derive boundary conditions from the Lagrangian/Hamiltonian with fundamental requirements and how the boundary condition parameters enter the description of electron states. With the benefit of boundary condition parameters, we can see topological structure and relation of bulk states and edge states clearly. This chapter is a review of [23], with some modification.

3.1 Lagrangian formalism of 3D Weyl semimetals and boundary conditions

Let us describe a generic and consistent boundary condition of a Weyl semimetal in 3+1 spacetime dimensions. Metric convention is chosen as $\eta_{\mu\nu} = \mathrm{diag}(+,-,-,-)_{\mu\nu}$.

The bulk Lagrangian (for a right-handed Weyl fermion) required by Hermiticity is written as

$$\mathcal{L} = \frac{i}{2}\psi^\dagger \sigma^\mu (\overrightarrow{\partial}_\mu - \overleftarrow{\partial}_\mu)\psi \tag{3.1}$$

where $\sigma^\mu = (\mathbf{1}_2, \sigma_1, \sigma_2, \sigma_3)$. The Dirac equation is

$$\sigma^\mu \partial_\mu \psi = 0 \tag{3.2}$$

which can be rewritten as

$$\left[i\partial_0 + i\sigma_i \partial_i\right]\psi = 0 \tag{3.3}$$

where $i = 1, 2, 3$. So the Hamiltonian is $i\partial_0 = \mathcal{H}_{\mathrm{bulk}}$,

$$\mathcal{H}_{\mathrm{bulk}} = p_1\sigma_1 + p_2\sigma_2 + p_3\sigma_3\,. \tag{3.4}$$

In order to study physics on the boundary of the material, let us introduce a surface term in the Lagrangian. This is a generic term which is one dimension lower than bulk. The action of Weyl fermion with a surface term is given by

$$S = \int_{x^3 \geq 0} d^3x \, \frac{i}{2} \psi^\dagger \sigma^\mu (\overrightarrow{\partial}_\mu - \overleftarrow{\partial}_\mu) \psi + \frac{1}{2} \int_{x^3=0} d^2x \, \psi^\dagger N \psi \, . \tag{3.5}$$

A variation $\psi \to \psi + \delta\psi$ and $\psi^\dagger \to \psi^\dagger + \delta\psi^\dagger$ provides equations at the surface $x^3 = 0$ as

$$\left[-i\psi^\dagger \sigma_3 + \psi^\dagger N\right] \delta\psi \Big|_{x^3=0} = 0, \quad \delta\psi^\dagger \left[i\sigma_3 \psi + N\psi\right] \Big|_{x^3=0} = 0. \tag{3.6}$$

The equations above become

$$\psi^\dagger \left[-i\sigma_3 + N\right] \delta\psi \Big|_{x^3=0} = 0, \quad \delta\psi^\dagger \left[i\sigma_3 + N\right] \psi \Big|_{x^3=0} = 0. \tag{3.7}$$

Let's study it with assuming N is hermitian. The two equations of (3.7) are Hermitian conjugate of each other. [1]

Since half of the modes on the boundary needs to be killed by the boundary condition. We can write generic boundary condition as

$$\begin{pmatrix} \alpha & \beta \end{pmatrix} \psi \Big|_{x^3=0} = 0 \, , \tag{3.8}$$

where α and β are constants. So $\psi\Big|_{x^3=0}$ should have the form

$$\psi \Big|_{x^3=0} = \begin{pmatrix} \beta \\ -\alpha \end{pmatrix} \xi \, , \tag{3.9}$$

and ξ is a Grassmann number. In the same manner,

$$\delta\psi \Big|_{x^3=0} = \begin{pmatrix} \beta \\ -\alpha \end{pmatrix} \delta\xi \, . \tag{3.10}$$

[1] The boundary condition obtained from assuming arbitrary $\delta\psi$ and $\delta\psi^\dagger$ to be arbitrary is too restricted. In such a case second equation in (3.7) becomes

$$(i\sigma_3 + N)\psi \Big|_{x^3=0} = 0.$$

Now the $\delta\psi$ satisfying above equation will lead to inconsistency: Combining

$$(i\sigma_3 + N)\delta\psi \Big|_{x^3=0} = 0,$$

with the first equation of (3.7), we get

$$-i\psi^\dagger \sigma_3 \delta\psi \Big|_{x^3=0} = 0 = \psi^\dagger N \delta\psi \Big|_{x^3=0}.$$

Then N has to be proportional to σ_3, otherwise there's no solution. In either case, the boundary conditions obtained do not depend on matrix N.

Parametrizing

$$N = \begin{pmatrix} n_0 + n_3 & n_1 - in_2 \\ n_1 - in_2 & n_0 - n_3 \end{pmatrix}, \tag{3.11}$$

together with (3.29) and (3.10) submitting into second equation of (3.7), we have

$$\begin{pmatrix} \beta^* & -\alpha^* \end{pmatrix} \begin{pmatrix} n_0 + n_3 + i & n_1 - in_2 \\ n_1 - in_2 & n_0 - n_3 - i \end{pmatrix} \begin{pmatrix} \beta \\ \alpha \end{pmatrix} \xi^\dagger \delta\xi = 0\,. \tag{3.12}$$

This becomes

$$|\beta|^2(n_0 + n_3 + i) - \beta^*\alpha(n_1 - in_2) - \alpha^*\beta(n_1 + in_2) + |\alpha|^2(n_0 - n_3 - i) = 0\,. \tag{3.13}$$

Now writing α and β explicitly as:

$$\begin{cases} \alpha = \rho_1 e^{-i\theta_1} \\ \beta = \rho_2 e^{i\theta_2}\,, \end{cases}$$

(3.13) becomes

$$(\rho_1^2 + \rho_2^2)n_0 + (\rho_1^2 - \rho_2^2)(n_3 + i) - 2\rho_1\rho_2(n_1\cos(\theta_1 + \theta_2) + n_2\sin(\theta_1 + \theta_2)) = 0\,. \tag{3.14}$$

Submitting (3.29) and (3.10) into the first equation of (3.7), and following the same procedure we have

$$(\rho_1^2 + \rho_2^2)n_0 + (\rho_1^2 - \rho_2^2)(n_3 - i) - 2\rho_1\rho_2(n_1\cos(\theta_1 + \theta_2) - n_2\sin(\theta_1 + \theta_2)) = 0\,. \tag{3.15}$$

Both (3.14) and (3.15) are solved by

$$\begin{cases} \rho_1^2 = \rho_2^2 \\ n_0 - n_1\cos(\theta_1 + \theta_2) + n_2\sin(\theta_1 + \theta_2) = 0\,, \end{cases} \tag{3.16}$$

these two equations tell us that the magnitudes of two components should be the same and phase of two components is different by $e^{-i(\theta_1+\theta_2)}$ as a function of n_0, n_1 and n_2. And we can write (3.8) as

$$\begin{pmatrix} 1 & e^{i(\theta_1+\theta_2)} \end{pmatrix} \psi\Big|_{x^3=0} = 0\,. \tag{3.17}$$

Let's determine this function. From the second equation of (3.16)we get

$$\cos(\theta_1 + \theta_2) = \frac{n_0 n_1}{n_1^2 + n_2^2} \mp \frac{n_2}{n_1^2 + n_2^2}\sqrt{n_1^2 + n_2^2 - n_0^2} \tag{3.18}$$

and

$$\sin(\theta_1 + \theta_2) = -\frac{n_0 n_2}{n_1^2 + n_2^2} \pm \frac{n_1}{n_1^2 + n_2^2}\sqrt{n_1^2 + n_2^2 - n_0^2}\,, \tag{3.19}$$

if

$$n_1^2 + n_2^2 - n_0^2 \geq 0\,. \tag{3.20}$$

This means that the phase difference of two component is

$$\begin{aligned} e^{-i(\theta_1+\theta_2)} &= \cos(\theta_1+\theta_2) - i\sin(\theta_1+\theta_2) \\ &= -\frac{n_0}{n_1+in_2} \mp \frac{i\sqrt{n_1^2+n_2^2-n_0^2}}{n_1+in_2}\,. \end{aligned} \tag{3.21}$$

As a result the boundary conditions become

$$\left(\begin{array}{cc} 1 & \frac{n_0}{n_1+in_2} \pm \frac{i\sqrt{n_1^2+n_2^2-n_0^2}}{n_1+in_2} \end{array} \right) \psi\Big|_{x^3=0} = 0\,. \tag{3.22}$$

In this case the boundary condition parameter completely depend on the surface parametrization.

3.2 Hamiltonian formalism and boundary conditions

In this section, I will derive generic boundary conditions in Hamiltonian formalism so the result will not be limited to classical level.

The Hermiticity condition of Hamiltonian is

$$\langle \mathcal{H}\psi_1 | \psi_2 \rangle = \langle \psi_1 | \mathcal{H}\psi_2 \rangle, \tag{3.23}$$

for arbitrary normalizable ψ_1 and ψ_2. The Hamiltonian is

$$\mathcal{H} = \mathcal{H}_{\text{bulk}} + \mathcal{H}_{\text{boundary}}\,, \tag{3.24}$$

where

$$\mathcal{H}_{\text{bulk}} = -i\sigma_i\partial_i \tag{3.25}$$

$$\mathcal{H}_{\text{boundary}} = K\delta(x^3)\,, \tag{3.26}$$

where K is a 2-by-2 Hermitian matrix. When we explicitly write the two inner product above as an integration, we find a surface difference between the right hand side and the left hand side, which must vanish, while the boundary Hamiltonian does not contribute:

$$[\psi_1^\dagger \sigma_3 \psi_2]\Big|_{x_3=0} = 0\,. \tag{3.27}$$

We can again write generic boundary condition as

$$\left(\begin{array}{cc} \alpha & \beta \end{array} \right) \psi\Big|_{x^3=0} = 0\,, \tag{3.28}$$

$\psi_i\Big|_{x^3=0}$, $i = 1, 2$ should have the form

$$\psi_i\Big|_{x^3=0} = \begin{pmatrix} \beta \\ -\alpha \end{pmatrix} \xi_i \,, \tag{3.29}$$

and ξ_i are Grassmann numbers.

Substituting (3.29) into (3.27)

$$\begin{pmatrix} \beta^* & -\alpha^* \end{pmatrix} \sigma_3 \begin{pmatrix} \beta \\ \alpha \end{pmatrix} \xi_1^\dagger \xi_2 = 0 \,, \tag{3.30}$$

The above equation gives

$$|\alpha|^2 = |\beta|^2 \,, \tag{3.31}$$

which means that α and β can only differ by a phase, from which we conclude that[2]

$$\begin{pmatrix} 1 & e^{-i\theta} \end{pmatrix} \psi\Big|_{x^3=0} = 0. \tag{3.32}$$

[2]We can use the same argument to derive boundary conditions of graphene with Hamiltonian

$$\mathcal{H}_{\text{bulk}} = p_1\sigma_1 + p_2\sigma_2 \,,$$

with boundary at for instance $x^2 = 0$. With the same argument of Hermiticity, then we have on the boundary

$$[\psi_1^\dagger \sigma_2 \psi_2]\Big|_{x_3=0} = 0 \,,$$

Using the parametrization which write generic boundary condition as

$$\begin{pmatrix} \alpha & \beta \end{pmatrix} \psi\Big|_{x^3=0} = 0 \,,$$

we get

$$\beta^*\alpha - \alpha^*\beta = 0 \,.$$

If $\alpha = \rho_1 e^{i\theta_1}$ and $\beta = \rho_2 e^{i\theta_2}$,we have that

$$\sin(\theta_1 - \theta_2) = 0$$

the components have same phase but different magnitude. So again the boundary condition of graphene depends on one parameter:

$$\begin{pmatrix} \rho_1 & \rho_2 \end{pmatrix} \psi\Big|_{x^3=0} = 0 \,.$$

3.3 Bulk and edge states

3.3.1 Generic edge modes and dispersions

Solving eigenstate equation

From previous section we see that Schrodinger equation and boundary condition for Weyl semimetal are

$$\begin{cases} -i\sigma_i\partial_i\psi = \epsilon\psi & (3.33) \\ \begin{pmatrix} 1 & e^{-i\theta} \end{pmatrix}\psi\Big|_{x^3=0} = 0\,, & (3.34) \end{cases}$$

Now we look for edge mode solution to eigenvalue equation (3.33). With an explicit two-component notation

$$\psi = \begin{pmatrix} \xi \\ \eta \end{pmatrix}, \tag{3.35}$$

the eigenstate equation (3.33) can be written as

$$\begin{pmatrix} -i\partial_3 - \epsilon & p_1 - ip_2 \\ p_1 + ip_2 & i\partial_3 - \epsilon \end{pmatrix}\begin{pmatrix} \xi \\ \eta \end{pmatrix} = 0. \tag{3.36}$$

This equation can be reorganized into two independent second-order differential equations:

$$\left(p_1^2 + p_2^2 - \epsilon^2 - \partial_3^2\right)\begin{pmatrix}\xi\\ \eta\end{pmatrix} = 0\,. \tag{3.37}$$

We look for the modes localized at the boundary. For the edge modes, we need

$$\alpha^2 \equiv p_1^2 + p_2^2 - \epsilon^2 > 0, \tag{3.38}$$

then the corresponding solutions required by the normalizability are

$$\begin{pmatrix}\xi\\ \eta\end{pmatrix} = e^{-\alpha(\epsilon)x^3}\begin{pmatrix}\xi_0\\ \eta_0\end{pmatrix}\,, \tag{3.39}$$

where ξ_0 and η_0 have no dependence on x^3. These are the edge modes, and in the following we determine the dispersion $\epsilon(p_1, p_2)$ and the relation between the components ξ_0 and η_0.

Dispersion relation

We combine the results from eigenvalue equation (3.33) and boundary condition (3.34) for edge eigen modes. Using the boundary condition (3.32), the edge state wave function is written as

$$\begin{pmatrix}\xi\\ \eta\end{pmatrix} = e^{-\alpha(\epsilon)x^3}\begin{pmatrix}1\\ e^{i\theta}\end{pmatrix}\,, \tag{3.40}$$

up to a normalization factor and a phase. Substituting this to the Hamiltonian eigen equation (3.36), we obtain

$$(i\alpha - \epsilon) + (p_1 - ip_2)e^{i\theta} = 0\,. \tag{3.41}$$

Substituting equations (3.38) and (3.39) into equation (3.36), we get one independent equation:

$$(i\alpha - \epsilon)\xi_0 + (p_1 - ip_2)\eta_0 = 0. \tag{3.42}$$

Looking at the real and the imaginary parts of this equation, we easily find

$$\epsilon = -p_1 \cos\theta - p_2 \sin\theta\,, \tag{3.43}$$
$$\alpha = p_1 \sin\theta - p_2 \cos\theta\,. \tag{3.44}$$

We can rewrite the above two equations in a compact way:

$$\begin{pmatrix} \epsilon \\ \alpha \end{pmatrix} = - \begin{pmatrix} \cos\theta & \sin\theta \\ -\sin\theta & \cos\theta \end{pmatrix} \begin{pmatrix} p_1 \\ p_2 \end{pmatrix}. \tag{3.45}$$

Interestingly, (3.45) shows that what the boundary parameter does is only rotating the momenta (p_1, p_2) into (ϵ, α), the energy and the inverse of edge mode decay width (penetration depth). Plotting the dispersion relation, we actually see in Fig. 3.1 that the edge dispersion is rotated against the (p_1, p_2) axes by the change of the boundary parameter θ.

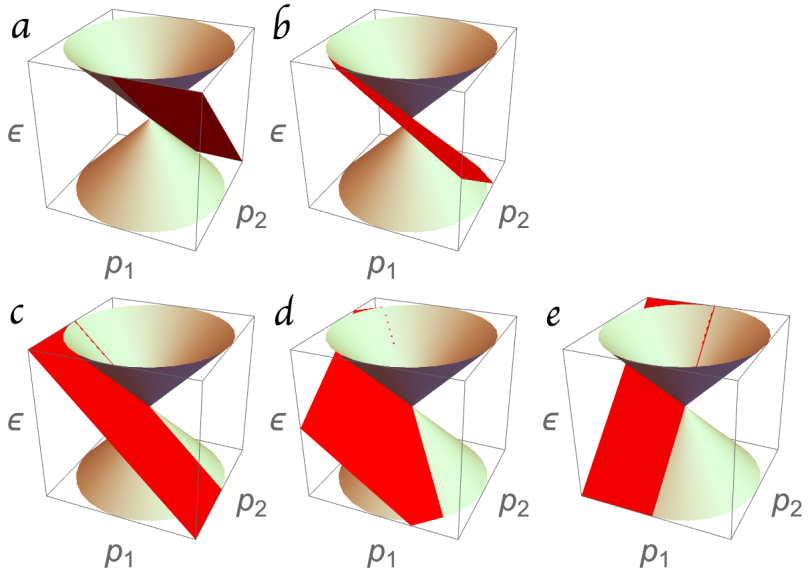

Figure 3.1: Figures a, b c, d, e respectively represent the energy dispersions of the bulk states and the edges states, for $\theta = \pi/2, \pi/4, 0, -\pi/4, -\pi/2$.

3.3.2 Wave function

Most of the information is used up and normalization condition is left only, from which the wave function is determined completely. Substituting (3.39) to the normalization condition

$$\int_0^\infty dx^3 \ \psi^\dagger \psi = 1, \tag{3.46}$$

we obtain a constraint

$$|\xi_0|^2 + |\eta_0|^2 = 2\alpha. \tag{3.47}$$

From the boundary condition (3.32), we can see that the two components should have the same magnitude with a difference of their phases. Combined with (3.47), they are determined up to an irrelevant overall phase:

$$\begin{pmatrix} \xi_0 \\ \eta_0 \end{pmatrix} = \sqrt{\alpha} \begin{pmatrix} e^{-i\theta} \\ -1 \end{pmatrix} . \tag{3.48}$$

So the general edge mode wave function is

$$\psi(x^3) = \sqrt{\alpha} \ \exp(-\alpha x^3) \begin{pmatrix} e^{-i\theta} \\ -1 \end{pmatrix}, \tag{3.49}$$
$$\alpha = p_1 \sin\theta - p_2 \cos\theta.$$

Note that the edge modes exist only in a limited region of the momentum space, since we need to require $\alpha > 0$. The linear inequality $\alpha > 0$ specifies a half of the momentum space, only in which the dispersion exists, see Fig. 3.1.

In the limit $\alpha = 0$, that is, on the line $p_1 \sin\theta - p_2 \cos\theta = 0$ in the momentum space, the edge mode approaches a non-normalizable mode, which is a constant wave function in the x^3 space. It corresponds to $p_3 = 0$ bulk mode, whose dispersion is $\epsilon = \pm\sqrt{p_1^2 + p_2^2}$, and $\epsilon \cos\theta = -p_1$; $\epsilon \sin\theta = -p_2$. So in fact, the edge dispersion (3.43) is identical to that under the condition $\alpha = 0$. Therefore we have a consistent picture for any value of θ: when the edge mode approaches a non-normalizable state in the momentum space, it is consistently and continuously absorbed into the bulk modes. In Fig. 3.1, we find explicitly that the edge dispersion surface has its boundary on the bulk dispersion surface.

In summary, we find that the dispersion of the edge state is attached to the bulk Weyl cone in such a way that (i) the edge dispersion is tangential to the Weyl cone, and (ii) the edge dispersion ends at the touching line on the Weyl cone.

3.4 Lattice models

3.4.1 Bulk lattice Hamiltonian

In this section we are going to consider lattice models of Weyl semimetals. The continuum model is regarded as an low energy effective description of lattice models. Yet, from the discussion below we will find that the same results like one-parameter dependence of boundary conditions, etc.

Our lattice version of Weyl semimetal can be written as

$$\mathcal{H}(p) = \sigma_1(\cos p_1 - \cos p_2 + c) + \sigma_2 \sin p_2 + \sigma_3 \sin p_3 \,, \tag{3.50}$$

because of the periodicity of momentum. This can be obtained from continuum model (3.4) by replacing p_i with $\sin p_i$, and as for p_1, we shift it into $p_1 + \pi/2$ such that two Weyl points will be symmetric with respect to the origin in the Brillouin zone. $\cos p_2$ is introduced to reduce the numbers of Weyl point. c is a free parameter and later we will see that by tuning c Weyl semimetal can be continuously deformed into gapped phase.

As a result, our tight-binding Hamiltonian is written as

$$H = \sum_n \psi_n^\dagger \mathcal{H} \psi_n \tag{3.51}$$

where n is a three-dimensional vector $n = (n_1, n_2, n_3) \in \mathbb{Z}^3$, and the operator $\mathcal{H}$ is given by

$$\begin{aligned} \mathcal{H} = \frac{1}{2}\sigma_1 \left(\nabla_1 + \nabla_1^\dagger - \nabla_2 - \nabla_2^\dagger + 2c\right) \\ - \frac{i}{2}\sigma_2 \left(\nabla_2 - \nabla_2^\dagger\right) - \frac{i}{2}\sigma_3 \left(\nabla_3 - \nabla_3^\dagger\right) \,, \end{aligned} \tag{3.52}$$

with difference operator defined by

$$\nabla_i \psi_n = \psi_{n+i} - \psi_n \,, \tag{3.53}$$

$$\nabla_i^\dagger \psi_n = \psi_{n-i} - \psi_n \,. \tag{3.54}$$

At Weyl points

$$\begin{aligned} \sqrt{(\cos p_1 - \cos p_2 + c)^2 + (\sin p_2)^2 + (\sin p_3)^2} \\ = -\sqrt{(\cos p_1 - \cos p_2 + c)^2 + (\sin p_2)^2 + (\sin p_3)^2} \end{aligned} \tag{3.55}$$

and the solutions are

$$(p_1^W, p_2^W, p_3^W) = \begin{cases} (\cos^{-1}(1-c), 0, 0 \;\&\; \pi) & (0 \le c \le 2) \\ (\cos^{-1}(-1-c), \pi, 0 \;\&\; \pi) & (-2 \le c \le 0) \\ \text{n/a} & (|c| > 2) \end{cases} . \tag{3.56}$$

Expanding the Hamiltonian around (p_1^W, p_2^W, p_3^W) we can get Weyl fermions:

$$\mathcal{H} \approx -\sigma_1 \sin p_1^W \delta p_1 + \sigma_2 \cos p_2^W \delta p_2 + \sigma_3 \cos p_3^W \delta p_3 \,. \tag{3.57}$$

At $c = 1$, $p_3^W = 0$, we can get two Weyl fermions:

$$\mathcal{H} \approx \mp \sigma_1 \delta p_1 + \sigma_2 \delta p_2 + \sigma_3 \delta p_3 \tag{3.58}$$

as a verification of continuum Hamiltonian.

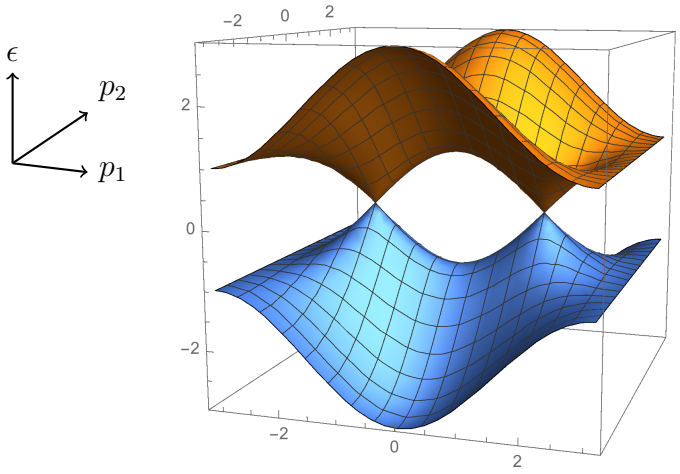

Figure 3.2: The energy band spectrum of the bulk Hamiltonian (3.50) with $p_3 = 0$ and $c = 1$. The Weyl points are at $(p_1, p_2) = (\pm\pi/2, 0)$.

3.4.2 Boundary conditions in lattice models

Now we introduce a boundary to this model and derive the boundary conditions. Hamiltonians including terms like $i\nabla^\dagger\psi_{n+1} = -i\nabla\psi_n$ is locally Hermitian. But just like the continuum Hamiltonian, the discrete Dirac Hamiltonians are also Hermitian up to the boundary term

$$\sum_{n=1}^{N} \psi_n^\dagger \left(-i\sigma\nabla\psi_n\right) + \psi_N^\dagger(i\sigma)\psi_{N+1} = \sum_{n=1}^{N} \left(i\sigma\nabla^\dagger\psi_n\right)^\dagger \psi_n - (i\sigma\psi_0)^\dagger\psi_1 \tag{3.59}$$

where we introduced auxiliary fields ψ_0 and ψ_{N+1}. So we have the following condition:

$$\psi_0^\dagger(i\sigma)\psi_1 - \psi_N^\dagger(i\sigma)\psi_{N+1} = 0\,. \tag{3.60}$$

We have two possibilities to solve this condition. The first is the periodic boundary condition $\psi_n = \psi_{n+N}$ for $\forall n \in \{1, \ldots, N\}$.Then these two terms cancel each other. The second is the situation that the both two terms vanish independently, which corresponds to the open boundary condition. Since we are interested in boundary effects, let's study open boundary conditions. Let us focus on the first term $\psi_0^\dagger(i\sigma)\psi_1$. Suppose the lattice is defined on the region $n_3 \geq 1$, the open boundary condition become $\psi_0^\dagger(i\sigma_3)\psi_1 = 0$. This is nothing but (3.27). We impose the boundary condition

$$(M+1)\,\psi\Big|_{n_3=1} = 0 \tag{3.61}$$

then we immediately get

$$M^\dagger\sigma_3 + \sigma_3 M = 0\,. \tag{3.62}$$

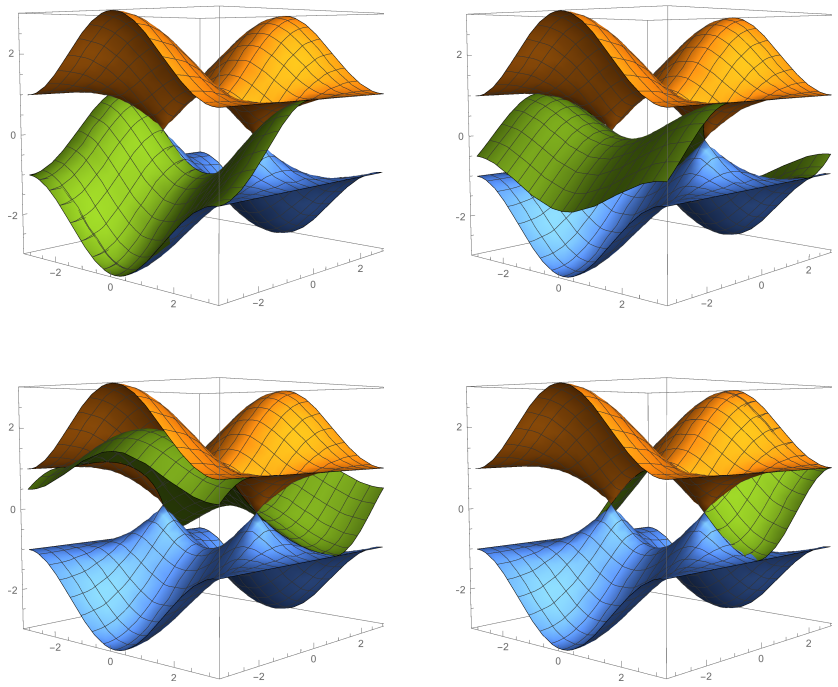

Figure 3.3: The dispersion relations of the bulk (orange and blue) and the edge (green) states with respect to the (p_1, p_2)-plane (horizontal) for positive β and $\theta = 0, \pi/3, 2\pi/3, \pi$.

Then the situation is completely parallel with the continuum theory studied in the previous section. Following the same procedure, we get boundary condition

$$\begin{pmatrix} 1 & e^{-i\theta} \end{pmatrix} \psi \Big|_{n_3=1} = 0\,, \tag{3.63}$$

which is equivalent to

$$\psi_{n_3=1} \propto \begin{pmatrix} 1 \\ -e^{i\theta} \end{pmatrix}\,. \tag{3.64}$$

Thus it depends only on the parameter θ in the end.

3.4.3 The dispersion and wave functions in lattice models

We consider the dispersion and wave function of the edge state with the boundary condition (3.64). For the eigenvalue equation

$$\mathcal{H}\psi = \epsilon(p)\psi\,, \tag{3.65}$$

the Hamiltonian has a matrix form in the partial Fourier basis,

$$\mathcal{H} = \begin{pmatrix} 0 & \Delta(p)^\dagger \\ \Delta(p) & 0 \end{pmatrix} - \frac{i}{2}\sigma_3 \left(\nabla_3 - \nabla_3^\dagger\right) \tag{3.66}$$

where the off-diagonal element is given by

$$\Delta(p) = \cos p_1 - \cos p_2 + c + i \sin p_2 \,, \tag{3.67}$$

which behaves as $\Delta(p) \sim \mp p_1 + i p_2$ in the vicinity of the Weyl points. The sign $\mp$ depends on the chirality of the Weyl points.

Assuming that the wavefunction is given by

$$\psi_{n_3} = \beta^{n_3 - 1} \psi_1 \tag{3.68}$$

in which the real parameter $|\beta| \leq 1$ plays as the role of $e^{-\alpha}$ in continuum theory, the eigenvalue equation (3.65) is equivalent to

$$D \psi_{n_3} = 0 \tag{3.69}$$

where

$$D = -\frac{i}{2} \begin{pmatrix} \beta^2 - 2i\epsilon(p)\beta - 1 & 2i\Delta(p)^\dagger \beta \\ -2i\Delta(p)\beta & \beta^2 + 2i\epsilon(p)\beta - 1 \end{pmatrix} . \tag{3.70}$$

To obtain a non-trivial solution to this zero mode equation, we asign the condition $\det D = 0$ which yields

$$\begin{aligned} \beta^2 = 1 &+ 2(|\Delta(p)|^2 - \epsilon(p)^2) \\ &- 2\sqrt{(|\Delta(p)|^2 - \epsilon(p)^2)(|\Delta(p)|^2 - \epsilon(p)^2 + 1)} \,. \end{aligned} \tag{3.71}$$

There are two solutions for $\beta \geq 0$ and $\beta \leq 0$. We remark that these two possibilities correspond to the doublers at $p_3 = 0$ and π in the momentum space.

Then, together with the boundary condition (3.64), the edge state equation (3.69) gives

$$D \begin{pmatrix} 1 \\ -e^{2i\theta} \end{pmatrix} = 0 \,. \tag{3.72}$$

Since $\beta \in \mathbb{R}$, we obtain

$$\epsilon(p) = -\cos\theta \,\mathrm{Re}\,\Delta(p) - \sin\theta \,\mathrm{Im}\,\Delta(p) \,, \tag{3.73}$$

$$\tilde{\alpha}(p) = \sin\theta \,\mathrm{Re}\,\Delta(p) - \cos\theta \,\mathrm{Im}\,\Delta(p) \,, \tag{3.74}$$

which is rewritten as a matrix form

$$\begin{pmatrix} \epsilon(p) \\ \tilde{\alpha}(p) \end{pmatrix} = - \begin{pmatrix} \cos 2\theta & \sin 2\theta \\ -\sin 2\theta & \cos 2\theta \end{pmatrix} \begin{pmatrix} \mathrm{Re}\,\Delta(p) \\ \mathrm{Im}\,\Delta(p) \end{pmatrix} , \tag{3.75}$$

where we define

$$\tilde{\alpha}(p) := \frac{1}{2} \left(\beta^{-1} - \beta \right) , \tag{3.76}$$

and from (3.67), the real and imaginary parts of $\Delta(p)$ are given by

$$\mathrm{Re}\,\Delta(p) = \cos p_1 - \cos p_2 + c\,, \tag{3.77}$$
$$\mathrm{Im}\,\Delta(p) = \sin p_2\,. \tag{3.78}$$

Comparing with the continuum theory (3.45), now the situation is parallel under the replacement

$$(p_1, p_2, \alpha(p)) \;\longrightarrow\; (\mathrm{Re}\,\Delta(p), \mathrm{Im}\,\Delta(p), \tilde{\alpha}(p))\;. \tag{3.79}$$

With (3.76) we can solve out β

$$\beta = -\sin\theta\,\mathrm{Re}\,\Delta(p) + \cos\theta\,\mathrm{Im}\,\Delta(p) + \sqrt{(\sin\theta\,\mathrm{Re}\,\Delta(p) - \cos\theta\,\mathrm{Im}\,\Delta(p))^2 + 1} \tag{3.80}$$

since $|\beta| \leq 1$. and hence

$$\psi_{n_3} = \beta^{n_3 - 1}\psi_1 \tag{3.81}$$

Fig. 3.3 shows the boundary parameter dependence of the bulk and edge state dispersions. The edge state spectrum has a support only where the normalizability conditioin is satisfied $|\beta| \leq 1$. As mentioned before, there are two solutions corresponding to positive and negative β. We focus on the positive solution in the following. When we change the parameter θ, the edge state spectrum rotates around the Weyl points. The orientation, that is, how the edge state spectrum winds, depends on the chirality of the Weyl nodes. This result is consistent with the continuum theory analysis in particular in the vicinity of the Weyl points.

To see the parameter dependence more explicitly, let us take the constant energy section of the spectrum, which yields the Fermi arc, shown in Figs. 3.4. This shows that the parameter characterizing the boundary condition θ plays a role of the rotation angle of the Fermi arc, as studied in continuum theory. In the present case of the lattice models, the Fermi arc ends on the Weyl points and have a finite support in the momentum space. Such a behavior of the Fermi arc has been experimentally observed, for example, in the transition metal pnictide family [9].

3.5 The bulk-edge correspondence

In this section, we study the relation between the bulk and the edge states, and check the bulk-edge correspondence under the change of boundary condition parameter. The bulk-edge correspondence [16, 14] for topological insulators is well-known, while that for 3D Weyl semimetals has been understood in a way through a dimensional reduction to 2D. Since the bulk-edge correspondence is a statement based on topology, we should expect that under the continuous change of parameters, the topological number do not change. Moreover, we may expect that boundary condition parameter can be used to interpret the topological number, and that is the case for Weyl semimetals. In the following subsections, we are going to explain the bulk-edge correspondence for the 3D Weyl semimetal, showing the topological

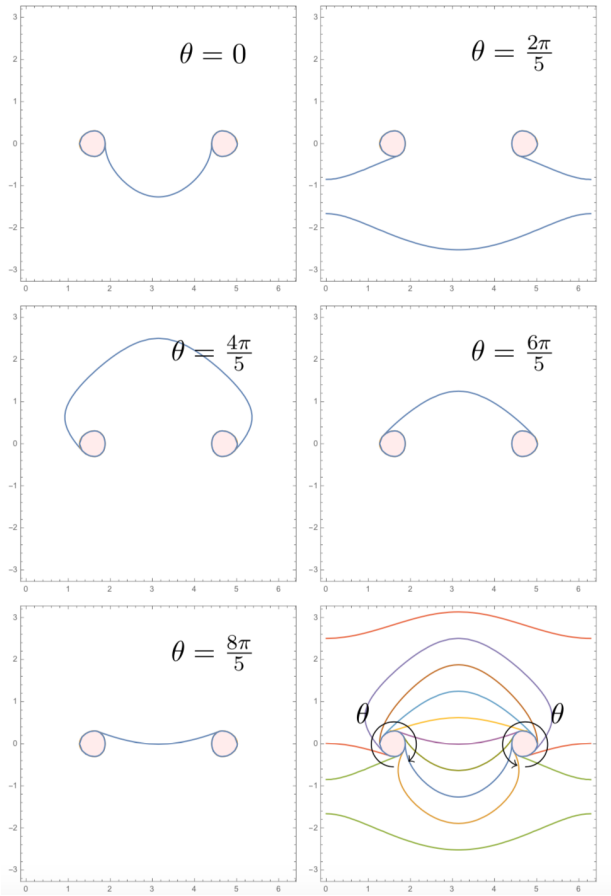

Figure 3.4: The parameter dependence of the Fermi arc which is the finite energy slice $\epsilon(p) = 0.3$ of the edge state energy spectrum with $\theta = 0, 2\pi/5, 4\pi/5, 6\pi/5, 8\pi/5$ for positive β. The horizontal and vertical axes are for p_1 and p_2. The shaded region shows the bulk spectrum. The last panel shows Fermi arcs with various parameter $\theta \in [0, \pi)$.

number is related with the rotation direction of Fermi-arc under the increasing of boundary parameter.

In three dimensions, the topological number K is defined by the wrapping number of a map $b_i(p_j)$ which shows up in the Hamiltonian

$$\mathcal{H} = b_i(p_j)\sigma_i. \tag{3.82}$$

Our Hamiltonian (3.4) is given by $b_i = p_i$ and the Weyl node is at $p_i = 0$. Considering a two-sphere surrounding the Weyl node, we obtain

$$K = 1 \in \pi_2(S^2). \tag{3.83}$$

We claim the bulk-edge correspondence for the 3D Weyl semimetal is given by

$$K = N - \tilde{N} \tag{3.84}$$

where K is the topological number defined above. We define N and $\tilde{N}$ to count the numbers of edge states with independent orientations with respect to the orientation of the bulk dispersion cone, as we will see below.

To discuss the orientation, we have to view the bulk dispersion in the subspace (p_1, p_2) since the edge dispersion lives in that space. First, in the (p_1, p_2, ϵ) space, we notice that all constant p_3 slices of the bulk states have the same orientation. Let us make further a slice at a constant positive energy ϵ. The cross-section of the bulk dispersion is a circle (see Fig. 4.1). The orientation of the circle is definite due to the topological number (assuming $b_3 = p_3$).

The constant energy slice of the edge dispersions defines the Fermi arcs. Since generically the edge state dispersions are planes tangent to the bulk dispersions, the Fermi arcs share the same property. The number N counts the number of Fermi arcs which are tangential to the bulk dispersion circle and emanates in a counter-clockwise orientation. On the other hand, the number $\tilde{N}$ counts that in a clockwise orientation. Our claim for the bulk-edge correspondence is that this orientation of the bulk circle remains the same for the edge (the Fermi arcs).

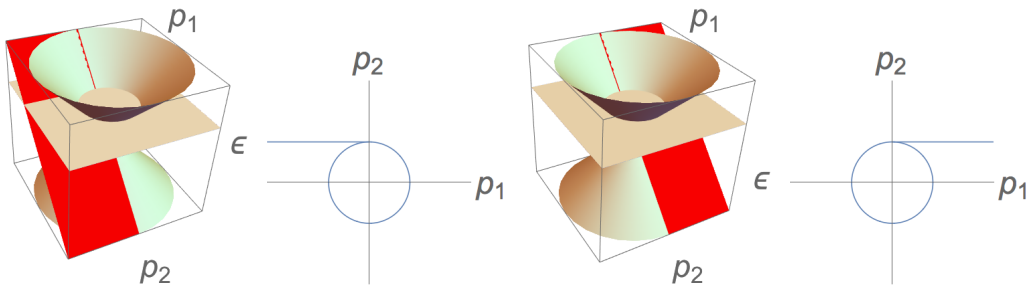

Figure 3.5: How to count the number of edge states from the orientation of the Fermi arcs. Top: a Fermi arc emanates from the Weyl node with a positive chirality $K = 1$, which is a counter-clockwise. Bottom: the case of the opposite chirality, $K = -1$.

Let us check this explicitly for two typical examples. In Fig. 4.1 we show the Hamiltonian (3.4) with $\theta = 0$, and the case of the Hamiltonian $\mathcal{H} = -p_1\sigma_1 + p_2\sigma_2 + p_3\sigma_3$ with $\theta = 0$. The former case has $K = 1$ as explained before, while the latter case has $K = -1$. As we can see in Fig. 4.1, it is obvious that we have $(N, \tilde{N}) = (1, 0)$ for the former case, and $(N, \tilde{N}) = (0, 1)$ for the latter case. So, they are consistent with our claim of the bulk-edge correspondence (3.84).

All the edge states in Fig. 3.1 have the same N and $\tilde{N}$ according to our definition: $(N, \tilde{N}) = (1, 0)$. So they are consistent again with (3.84). The examples in the lattice models we considered are shown to be consistent with the bulk-edge correspondence. Note that Fermi arcs join Weyl nodes, and our counting works for each Weyl node. To be more precise, each Fermi arc has two end points, and one end has $(N, \tilde{N}) = (1, 0)$ while the other end has $(N, \tilde{N}) = (0, 1)$. So the numbers are assigned to each end point of the Fermi arc.

Chapter 4

Analysis in 5D Weyl semimetals

In general, band-crossing happens between two bands, so even if there are many bands, we can always focus on the two band in which band-crossing occurs while ignoring other bands. So the bulk picture of topological phases in multi-band systems is essentially the same as in two-band system. However, the boundary picture is so much different as the boundary parameter increases in number. In this chapter, we will see even with a very simple four-band Hamiltonian — 5D Weyl semimetal, an enriched boundary parameter space and a new exotic state — edge-of-edge state come out. This chapter is mainly based on [24] but I add more examples of edge state and edge of edge state dispersions. The relation between gapped bulk, gapped edge, and gapless edge-of-edge states is also appearing in [25], where explicit experimental realization is proposed.

4.1 5D Weyl semimetals, Hamiltonian, Lagrangian

To consider topological phases with four bands, the easiest way is to generalize Hamiltonians from lower dimensions to higher dimensions. The straight forward generalization is from 3+1 dimensional Weyl semimetal into 5+1 dimensional Weyl semimetal. Since they are chiral, automatically they have topological property and by dimensional reduction, they are related with topological insulators in lower dimensions. 5D Weyl semimetals have the Hamiltonian of form

$$\mathcal{H} = \sum_{M=1}^{5} \Gamma^M p_M \tag{4.1}$$

as in the same manner as the standard Weyl semimetal Hamiltonian $\mathcal{H} = p_1\sigma_1 + p_2\sigma_2 + p_3\sigma_3$ in 1+3 spacetime dimensions. Here Γ^M $(M = 1, \cdots, 5)$ is the 4×4 Gamma matrix satisfying the 5-dimensional Euclidean Clifford algebra

$$\{\Gamma^M, \Gamma^N\} = 2\delta^{MN} \quad (M, N = 1, 2, 3, 4, 5)\,. \tag{4.2}$$

This kind of band Hamiltonian has topological property in the bulk since it's chiral in 5+1 dimensions. Let's check it. It is parallel to the calculation done in 3 dimensions.

The winding number is given by the formula

$$\begin{aligned}\omega(S_\alpha) &= \frac{1}{\int_{S_\alpha} d\Omega}\int_{S_\alpha=\partial M_\alpha} d^4p\ \epsilon^{1234}\epsilon^{abcde}\frac{p_a}{p}\partial_1\frac{p_b}{p}\partial_2\frac{p_c}{p}\partial_3\frac{p_d}{p}\partial_4\frac{p_e}{p} \\ &= \frac{1}{4!\int_{S_\alpha} d\Omega}\int_{M_\alpha} d^5p\ \partial_\lambda(\epsilon^{\lambda\mu\nu\alpha\beta}\epsilon^{abc}\frac{p_a}{p}\partial_\mu\frac{p_b}{p}\partial_\nu\frac{p_c}{p}\partial_3\frac{p_d}{p}\partial_4\frac{p_e}{p})\,. \end{aligned} \tag{4.3}$$

Again by using

$$\partial_\mu\frac{p_b}{p} = \frac{\delta_{\mu b}}{p} - \frac{p_\mu p_b}{p^3}\,, \tag{4.4}$$

(4.3) becomes

$$\omega(S_\alpha) = \frac{1}{4!\int_{S_\alpha} d\Omega}\int_{M_\alpha} d^5p\ \partial_\lambda(\epsilon^\lambda_{bcde}\epsilon^{abcde}\frac{p_a}{p^3}) = 1\,. \tag{4.5}$$

Upon a dimensional reduction to 4+1 dimensions by replacing p_5 by a constant m, the system reduces to the class A topological insulator in 4 dimensions with the Hamiltonian

$$\mathcal{H} = p_i\Gamma^i + m\Gamma^5\,. \tag{4.6}$$

Let's have a look at Lagrangian formalism formulation. The bulk Lagrangian is written in the same manner as the 1+3-dimensional case. Now with the gamma matrices in 4+1 dimensions,

$$\mathcal{L} = -\psi^\dagger i\gamma^0(\gamma^\mu\partial_\mu - i\partial_5)\psi \tag{4.7}$$

with $\bar\psi \equiv \psi^\dagger i\gamma^0$. Here $\mu = 0,1,2,3,4$ and the 4×4 gamma matrices are a representation of the Clifford algebra $\{\gamma^\mu,\gamma^\nu\} = 2\eta^{\mu\nu}$ $(\mu,\nu = 0,1,2,3,4)$. Note that the Gamma matrices γ^μ are a part of 8×8 Gamma matrices in $1+5$ dimensions. The Dirac equation is

$$(\gamma^\mu\partial_\mu - i\partial_5)\psi = 0 \tag{4.8}$$

which can be rewritten as

$$\left[i\partial_0 - i\gamma^0(\gamma^i\partial_i - i\partial_5)\right]\psi = 0 \tag{4.9}$$

where $i = 1,2,3,4$. So the Hamiltonian is $i\partial_0 = \mathcal{H}$,

$$\mathcal{H} \equiv -\gamma^0\gamma^i p_i + i\gamma^0 p_5\,. \tag{4.10}$$

We have used $p_i = -i\partial_i$ and $p_5 = -i\partial_5$. If we use a redefined Gamma matrices

$$\Gamma^5 \equiv i\gamma^0, \quad \Gamma^i \equiv -\gamma^0\gamma^i \tag{4.11}$$

then they satisfy (4.2). And the Hamiltonian is conveniently written as (4.1). Meanwhile, we can define another set of Gamma matrices, such that

$$\Gamma'^5 \equiv -i\gamma^0, \quad \Gamma'^i \equiv \gamma^0\gamma^i \tag{4.12}$$

and they also satisfy the same algebra as (4.2), however, the Hamiltonian will then be written as

$$\mathcal{H} = \sum_{M=1}^{5} \Gamma'^M(-p_M)\,. \tag{4.13}$$

These two kinds of Hamiltonians describe fermions with two opposite chirality in 5+1 dimensions, therefore they are called Weyl fermions. If formula (4.3) is used, winding number $\omega = -1$ is obtained.

4.2 Generic boundary conditions and edge states

4.2.1 Boundary conditions

The boundary condition is imposed at $x^5 = 0$,

$$A\psi = 0\,. \tag{4.14}$$

Again defining $A = M + \mathbb{1}_4$, we have

$$M\psi = -\psi\,. \tag{4.15}$$

One of the eigen value of A is vanishing.

The boundary condition receive another constraint from the Hermiticity of Hamiltonian just as the discussion in Sect. 3.1.

The Hermiticity condition of Hamiltonian is

$$\langle \mathcal{H}\psi_1 | \psi_2 \rangle = \langle \psi_1 | \mathcal{H}\psi_2 \rangle, \tag{4.16}$$

for arbitrary normalizable ψ_1 and ψ_2. The Hamiltonian is

$$\mathcal{H} = \mathcal{H}_{\text{bulk}} + \mathcal{H}_{\text{boundary}}\,, \tag{4.17}$$

where

$$\mathcal{H}_{\text{bulk}} = -i\Gamma_M\partial_M \tag{4.18}$$

$$\mathcal{H}_{\text{boundary}} = N\delta(x^5)\,. \tag{4.19}$$

Then the Hermiticity requires a surface term to vanish

$$\psi_1^\dagger \Gamma^5 \psi_2 = 0\,, \tag{4.20}$$

just like (3.27).

We use the following representation of the Clifford algebra,

$$\Gamma^i = \begin{pmatrix} 0 & -i\sigma_i \\ i\sigma_i & 0 \end{pmatrix}, \tag{4.21a}$$

$$\Gamma^4 = \begin{pmatrix} 0 & \mathbb{1}_2 \\ \mathbb{1}_2 & 0 \end{pmatrix}, \quad \Gamma^5 = \begin{pmatrix} \mathbb{1}_2 & 0 \\ 0 & -\mathbb{1}_2 \end{pmatrix}. \tag{4.21b}$$

Then, decomposing $\psi_1 = (\xi_1, \eta_1)^T$ and $\psi_2 = (\xi_2, \eta_2)^T$, (4.20) is equivalent to

$$\xi_1^\dagger \xi_2 - \eta_1^\dagger \eta_2 = 0\,. \tag{4.22}$$

This equation is satisfied only if

$$\eta_1 = U_5 \xi_1\,, \quad \eta_2 = U_5 \xi_2\,, \tag{4.23}$$

for an arbitrary $U(2)$ matrix U_5. So, we conclude that the consistent generic solution of the boundary condition (4.20) is

$$\psi \propto \begin{pmatrix} \mathbb{1}_2 \\ U_5 \end{pmatrix} \xi \tag{4.24}$$

for a normalized two-spinor ξ. We remark that it can be reparametrized using $U(2)$ rotation, $\xi \to V\xi$ with $V \in U(2)$. In other words, the boundary condition is rephrased to

$$\left(\mathbb{1}_2 \;\; -U_5^\dagger\right) \psi\Big|_{x^5=0} = 0\,. \tag{4.25}$$

This condition is analogous to the 1+3-dimensional case (3.32). We notice that the previous $e^{i\theta}$ is replaced by the $U(2)$ unitary matrix $-U_5^\dagger$. We have four real parameters to parametrize the generic boundary condition and this fact does not depend on the basis we choose.

The condition (4.25) can be written in an alternative manner. Notice that it is equivalent to

$$\begin{pmatrix} \mathbb{1}_2 & -U_5^\dagger \\ U_5 & -\mathbb{1}_2 \end{pmatrix} \psi\Big|_{x^5=0} = 0\,. \tag{4.26}$$

There may be other expressions for N which reproduces (4.25), as in the case of the 3D Weyl semimetals.

4.2.2 Edge state

IN this section I will derive the dispersion relations. The bulk Hamiltonian eigen equation for $\psi = (\xi, \eta)^T$ is

$$(-i\partial_5 - \epsilon)\xi + (-i\sigma_i p_i + p_4)\,\eta = 0 \tag{4.27}$$

$$(i\sigma_i p_i + p_4)\,\xi - (-i\partial_5 + \epsilon)\eta = 0 \tag{4.28}$$

with $i = 1, 2, 3$. The edge state solution to the bulk Hamiltonian eigen equation is

$$\psi = \begin{pmatrix} \xi(p_i, p_4) \\ \eta(p_i, p_4) \end{pmatrix} \exp[-\alpha_5 x^5] \,, \quad \alpha_5 \equiv \sqrt{-\epsilon^2 + p_i^2 + p_4^2} \,. \tag{4.29}$$

Let us substitute the boundary condition (4.24). Then the equations (4.27) and (4.28) are written as

$$[(i\alpha_5 - \epsilon) + (-i\sigma_i p_i + p_4)\, U_5]\, \xi = 0 \,, \tag{4.30}$$
$$[-(i\alpha_5 + \epsilon) U_5 + (i\sigma_i p_i + p_4)]\, \xi = 0 \,. \tag{4.31}$$

Noting that the unitary matrix U_5 determining the boundary condition can be decomposed as

$$U_5 = e^{i\theta_5} U_5' \tag{4.32}$$

where U_5' is an $SU(2)$ matrix, and this acts as a rotation in the 4-dimensional momentum space,

$$(-i\sigma_i p_i + p_4)\, U_5' = -i\sigma_i \tilde{p}_i + \tilde{p}_4 \tag{4.33}$$

with

$$p_i^2 + p_4^2 = \tilde{p}_i^2 + \tilde{p}_4^2 \,. \tag{4.34}$$

Expanding (4.33) explicitly with

$$U_5' = a_0 \mathbb{1}_2 + i a_i \sigma^i, \quad a_0^2 + a_i^2 = 1, \ i = 1, 2, 3 \,, \tag{4.35}$$

we get

$$\begin{cases} \tilde{p}_4 = a_0 p_4 + a_i p_i \,, & (4.36) \\ \tilde{p}_i = a_0 p_i - a_i p_4 + \epsilon_{ijk} a_j p_k \,, & (4.37) \end{cases}$$

so this U_5' indeed acts as a rotation between four momenta. Then the two equations (4.30) and (4.31) in terms of rotated momenta are

$$\left[e^{-i\theta_5}(i\alpha_5 - \epsilon) + \tilde{p}_4 - i\sigma_i \tilde{p}_i\right] \xi = 0 \,, \tag{4.38}$$
$$\left[-e^{i\theta_5}(i\alpha_5 + \epsilon) + \tilde{p}_4 + i\sigma_i \tilde{p}_i\right] \xi = 0 \,. \tag{4.39}$$

Equivalently,

$$[\alpha_5 \sin\theta_5 - \epsilon \cos\theta_5 + \tilde{p}_4]\, \xi = 0 \,, \tag{4.40}$$
$$[\alpha_5 \cos\theta_5 + \epsilon \sin\theta_5 - \sigma_i \tilde{p}_i]\, \xi = 0 \,. \tag{4.41}$$

This has a solution only when

$$\alpha_5 \sin\theta_5 - \epsilon \cos\theta_5 + \tilde{p}_4 = 0 \,, \tag{4.42}$$
$$\det\left[\alpha_5 \cos\theta_5 + \epsilon \sin\theta_5 - \sigma_i \tilde{p}_i\right] = 0 \,. \tag{4.43}$$

The second equation implies

$$\alpha_5 \cos\theta_5 + \epsilon \sin\theta_5 = \pm\sqrt{\tilde{p}_i^2}\,. \tag{4.44}$$

So we finally obtain the dispersion relation of the edge state,

$$\epsilon = \tilde{p}_4 \cos\theta_5 \pm \sqrt{\tilde{p}_i^2}\sin\theta_5\,, \tag{4.45}$$

$$\alpha_5 = -\tilde{p}_4 \sin\theta_5 \pm \sqrt{\tilde{p}_i^2}\cos\theta_5\,. \tag{4.46}$$

The normalizability condition is $\alpha_5 > 0$ which constrains the momentum region for the existence of the edge state.

4.2.3 Some examples

Example 1

There is a similarity to the 1+3-dimensional case of the standard Weyl semimetals, (3.43) and (3.44). In fact, identifying $\theta = \theta_5 + \pi$ and putting $p_2 = p_3 = 0$ with $U_5' = \mathbb{1}_2$ means a consistent reduction from 1+5 dimensions to 1+3 dimensions, reproducing all the results of the three-dimensional Weyl semimetals. This is the U(1) part of the U(2).

Example 2

Next let's have a look at the SU(2) rotation. In U_5 if we choose

$$a_0 = \cos\alpha\,,\ a_1 = \sin\alpha\,,\ a_2 = a_3 = 0\,, \tag{4.47}$$

we get an explicit form of dispersion:

$$\epsilon = (p_4\cos\alpha + p_1\sin\alpha)\cos\theta_5 \pm \sqrt{(p_1\cos\alpha - p_4\sin\alpha)^2 + p_2^2 + p_3^2}\sin\theta_5\,. \tag{4.48}$$

We can see from this dispersion that p_1 and p_4 get rotated and that p_2 and p_3 are unchanged. If we choose

$$a_2 = \cos\alpha\,,\ a_3 = \sin\alpha\,,\ a_1 = a_0 = 0\,, \tag{4.49}$$

we get another explicit form of dispersion:

$$\epsilon = (p_2\cos\alpha + p_3\sin\alpha)\cos\theta_5 \pm \sqrt{(p_2\sin\alpha - p_3\cos\alpha)^2 + p_1^2 + p_4^2}\sin\theta_5\,. \tag{4.50}$$

p_2, p_3 and p_4 get rotated and p_1 is unchanged. It's clear from (4.36) and (4.37) that p_4 always gets rotated unless there's no rotation at all. These two cases are interesting for topological insulators related through dimensional reduction. By tuning θ, we can clearly get gapped or gapless edge states.

Example 3

If we choose

$$\theta_5 = \frac{\pi}{2} \text{ or } \frac{3\pi}{2} \tag{4.51}$$

we get

$$\epsilon = \pm\sqrt{\tilde{p}_i^2} = \pm\sqrt{(a_0 p_i - a_i p_4 + \epsilon_{ijk} a_j p_k)^2}\,. \tag{4.52}$$

They are edge states that can be gapped if some of the momenta are chosen to be constant.

And if we choose

$$\theta_5 = 0 \tag{4.53}$$

we get linear gapless edge states:

$$\epsilon = a_0 p_4 + a_i p_i \tag{4.54}$$

.

4.3 Intersection of boundaries: edge-of-edge states

The advantage of the four band Hamiltonian is the rich structure of the boundary condition parameter space such that the intersection of two boundary still have nontrivial parameter space and this provides the environment for the existence of edge-of-edge states. Furthermore, as we will argue soon that the edge states of the 5D Weyl semimetal have topological charges, at the edge of these edge states, it's natural that edge-of-edge states will appear. In this section, we will work out the edge-of-edge states explicitly.

4.3.1 Topological charge in the momentum space

In [21], a certain edge state appearing in a class A topological insulator in 1+4 dimensions was shown to possess a topological charge. As argued earlier, we note here that the 5D Weyl semimetal Hamiltonian reduces to a 4d class A topological insulator by a trivial dimensional reduction. So, it is natural that our generic edge state explored in the previous section has the same topological charge that was argued in [21].

In fact, it is easy to see the topological charge of the edge state. The topological charge is defined by a Berry connection of the wave function of the edge state. Recall that the edge state wave function is subject to the two equations (4.40) and (4.41). In particular the second equation (4.41) is recast to the form

$$\sigma_i \tilde{p}_i \xi = \pm\sqrt{\tilde{p}_i^2}\,\xi\,. \tag{4.55}$$

This has the same form as Hamiltonian of the 3D Weyl semimetal, (3.33). Therefore, the Berry connection of the edge state has a topological charge. It is identical to the chirality of the corresponding Weyl semimetal, in the rotated momentum frame spanned by $\tilde{p}_{1,2,3}$.

The topological charge in the momentum space for the edge state immediately means that there should appear an edge-of-edge state once a boundary of the edge is introduced properly.

4.3.2 Generic edge-of-edge states

Let us study the intersection of boundary $x^4 = 0$ and $x^5 = 0$ as the edge-of-edge of the material. The expected wave function should be of the form

$$\psi = \begin{pmatrix} \mathbb{1}_2 \\ U_5 \end{pmatrix} \chi(p_i) \exp[-\alpha_4 x^4 - \alpha_5 x^5] \,, \tag{4.56}$$

but at the same time satisfying boundary condition on $x^4 = 0$ (see Appendix A.1 for derivation)

$$\begin{pmatrix} \mathbb{1}_2 + U_4^\dagger & \mathbb{1}_2 - U_4^\dagger \end{pmatrix} \psi \Big|_{x^4=0} = 0 \,. \tag{4.57}$$

Therefore we demand

$$[U_5(\mathbb{1}_2 - U_4) - (\mathbb{1}_2 + U_4)] \, \chi = 0 \,. \tag{4.58}$$

The is is the compatibility condition with boundary condition (4.57). For that to have a nontrivial solution, we need

$$\det [\mathbb{1}_2 + U_4 - U_5 + U_5 U_4] = 0 \,. \tag{4.59}$$

This is a necessary condition for the existence of the edge-of-edge state. [1] Let's solve the existence condition (4.59) for the boundary conditions. We define

$$U_5 = e^{i\theta_5}(a_0 \mathbb{1}_2 + i a_i \sigma^i) = A_0 \mathbb{1}_2 + A_i \sigma^i \,, \tag{4.61a}$$

$$U_4 = e^{i\theta_4}(b_0 \mathbb{1}_2 + i b_i \sigma^i) = B_0 \mathbb{1}_2 + B_i \sigma^i \,. \tag{4.61b}$$

The unitarity of U_4 and U_5 means

$$a_0^2 + a_i^2 = b_0^2 + b_i^2 = 1 \,. \tag{4.61c}$$

[1] We remark that the condition (4.58) is covariant under the rotation

$$(U_4, U_5, \chi) \longrightarrow (W U_4 W^\dagger, W U_5 W^\dagger, W\chi) \tag{4.60}$$

with $W \in U(2)$. So there is an equivalence class of the edge-of-edge states related by this W.

After some computations, (4.59) becomes (see Appendix A.2)

$$\begin{aligned} a_0 = b_0 = 0\,, \quad a_i^2 = b_i^2 = 1\,, \\ a_i b_i = -\cos\theta_4 \cos\theta_5\,. \end{aligned} \tag{4.62}$$

This defines the parameter space of the edge-of-edge state.

Next let's solve the Hamiltonian eigen equation and obtain the dispersion of edge-of-edge states. The Hamiltonian eigen equation leads to

$$\left[(i\alpha_4 - \epsilon) + (-i\sigma_i p_i - i\alpha_5)\, U_4\right]\chi = 0\,, \tag{4.63}$$

$$\left[-(i\alpha_4 + \epsilon)U_4 + (i\sigma_i p_i - i\alpha_5)\right]\chi = 0\,. \tag{4.64}$$

Together with

$$\epsilon^2 = p_i^2 - \alpha_4^2 - \alpha_5^2\,, \tag{4.65}$$

we have three equations with three unknowns $(\epsilon, \alpha_4, \alpha_5)$ so they are solved and determine the edge-of-edge state dispersion. Together with (4.62), we get a consistency relation for the dispersion $\epsilon(p)$ of the generic edge-of-edge state to satisfy,

$$A\epsilon^2 - 2B\epsilon + C = 0\,, \tag{4.66}$$

where the coefficients are defined as

$$A \equiv 1 - \cos_4^\theta \cos_5^\theta\,, \tag{4.67a}$$

$$B \equiv a_i p_i \cos\theta_5 \sin_4^\theta + b_i p_i \cos\theta_4 \sin_5^\theta\,, \tag{4.67b}$$

$$C \equiv (a_i p_i)^2 \sin_4^\theta + (b_i p_i)^2 \sin_5^\theta - p_i^2 \sin_5^\theta \sin_4^\theta\,. \tag{4.67c}$$

See Appendix A.2 for details of the derivation.

4.3.3 Examples of edge-of-edge states

Let's now study some solutions of (4.66), as they are very interesting.

Example 1

As in Sec. 4.2.3, we can choose

$$\theta_4 = \theta_5 = \frac{\pi}{2} \text{ or } \frac{3\pi}{2}\,, \tag{4.68}$$

and easily get edge states that is gappable for dimensional reduced models. Now let's see what the edge-of-edge states dispersion look like. In such a case,

$$\begin{aligned} A = 1\,,\ B = 0\,, \\ C = (a_i p_i)^2 + (b_i p_i)^2 - p_i^2 \le 0\,, \end{aligned} \tag{4.69}$$

(thanks to (4.62)), so we have dispersion:

$$\epsilon_{\text{e-o-e}} = \pm\sqrt{p_i^2 - (a_i p_i)^2 - (b_i p_i)^2} = c_i p_i \,, \tag{4.70}$$

where

$$c_i^2 = 1,\ c_i a_i = c_i b_i = 0 \,. \tag{4.71}$$

The lesson from above is that edge-of-edge states are always linearly dependent on p_i , so they are always gapless, even after dimensional reduction to three or four spacial dimensions. This conclusion is very important for the discussion in the next subsection.

Example 2

If we set instead

$$\theta_5 = 0 \,, \tag{4.72}$$

we get

$$\begin{aligned} &A = 1 - \cos_4^\theta \,,\ B = a_i p_i \sin_4^\theta \,, \\ &C = (a_i p_i)^2 \sin_4^\theta \,, \end{aligned} \tag{4.73}$$

so the edge-of-edge state dispersion is

$$\epsilon_{\text{e-o-e}} = a_i p_i \,, \tag{4.74}$$

but this is exactly the same as edge states at $x^5 = 0$ (4.54): Since now $a_0 = 0$

$$\epsilon_{x^5=0} = a_i p_i \,, \tag{4.75}$$

one merge with another. The same result happen for boundary $x^4 = 0$ if we set

$$\theta_4 = 0 \,. \tag{4.76}$$

4.3.4 Reduction to 3d chiral topological insulator (class AIII)

Based the examples with gapless edge-of-edge states in the previous subsection, I'll discuss the dimensionally reduced model, which is a three-dimensional chiral topological insulator (class AIII) towards an experimental realization of the edge-of-edge state. See, for example, [26] for a setup of the class AIII system using ultracold atoms.

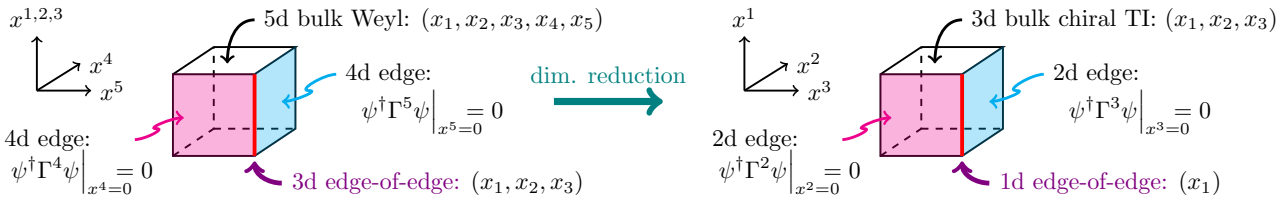

Figure 4.1: Edge-of-edge at 5D and dimensional reduced one 3D

Edge-of-edge state at $x^{2,3} = 0$

In order to study the edge-of-edge state in the 3d model, let me first show the edge states of the 5d Weyl fermion (4.1) at the boundaries $x^2 = 0$ and $x^3 = 0$. Later the fourth and fifth momenta will be set to constants. The boundary condition is imposed as

$$\psi^\dagger\Gamma^a\psi\Big|_{x^a=0} = 0 \quad (a = 2, 3)\,. \tag{4.77}$$

The edge state and the corresponding spectrum for this boundary condition is discussed in Appendix A.1 in details. The edge-of-edge state localized at the corner $x^2 = x^3 = 0$ is

$$\psi = e^{-\alpha_2 x^2 - \alpha_3 x^3} \begin{pmatrix} \mathbb{1}_2 + i\sigma_3 U_3 \\ i\sigma_3\left(\mathbb{1}_2 - i\sigma_3 U_3\right) \end{pmatrix} \xi \tag{4.78}$$

with the compatibility condition

$$\begin{aligned} \det\Big(&\mathbb{1}_2 + iU_2^\dagger\sigma_2 + i\sigma_3 U_3 - U_2^\dagger(i\sigma_1)U_3 \\ &+ i\sigma_1 - i\sigma_2 U_3 - iU_2^\dagger\sigma_3 - U_2^\dagger U_3\Big) = 0 \end{aligned} \tag{4.79}$$

since the boundary conditions (4.77) are rephrased as (A.7).

A solution to the compatibility condition (4.79) is

$$U_2 = \sigma_2\,, \quad U_3 = i\mathbb{1}_2\,, \tag{4.80}$$

which leads to

$$(\tilde{p}_1^{(a)}, \tilde{p}_2^{(a)}, \tilde{p}_3^{(a)}, \tilde{p}_4^{(a)}) = \begin{cases} (-p_3, p_4, p_1, p_5) & (a = 2) \\ (p_1, p_2, -p_5, p_4) & (a = 3) \end{cases} \tag{4.81}$$

with $\theta_2 = \theta_3 = \pi/2$. Thus the edge state spectrum is given by

$$\epsilon_2(p) = \pm\sqrt{p_1^2 + p_3^2 + p_4^2}\,, \tag{4.82a}$$

$$\epsilon_3(p) = \pm\sqrt{p_1^2 + p_2^2 + p_5^2}\,, \tag{4.82b}$$

and the corresponding edge-of-edge state spectrum is gapless and also chiral,

$$\epsilon = -p_1\,. \tag{4.83}$$

3d class AIII topological insulator

The Hamiltonian for the class AIII topological insulator has the following form

$$\mathcal{H}(\vec{p}) = \vec{p}\cdot\vec{\Gamma} + m\Gamma_4\,, \tag{4.84}$$

which is obtained from the 5d Weyl Hamiltonian (4.1) through the dimensional reduction $(p_4, p_5) \to (m, 0)$. The Γ-matrices (4.21) are expressed as

$$\Gamma^i = \tau_2 \otimes \sigma_i\,, \quad \Gamma^4 = \tau_1 \otimes \mathbb{1}_2\,, \quad \Gamma^5 = \tau_3 \otimes \mathbb{1}_2 \tag{4.85}$$

where the Pauli matrices σ's and τ's act on the spin $(\uparrow, \downarrow)$ and sublattice (A, B) degrees of freedom. Since the Hamiltonian anticommutes with Γ^5 as

$$\{\mathcal{H}(\vec{p}), \Gamma^5\} = 0\,, \tag{4.86}$$

for each eigenstate ψ_n of $\mathcal{H}$, in which

$$\mathcal{H}\psi_n = E_n\psi_n\,, \tag{4.87}$$

there is a state with same energy of opposite sign

$$\mathcal{H}\Gamma_5\psi_n = -\Gamma_5\mathcal{H}\psi_n = -E_n\Gamma_5\psi_n \tag{4.88}$$

and this is called the chiral (sublattice) symmetry.

We can apply the same boundary analysis to the dimensionally reduced model. Given a two-spinor denoted by $|\xi\rangle$, and choosing the boundary condition (4.80), we obtain

$$\psi(x^2 = 0) \propto \begin{pmatrix} \mathbb{1}_2 \\ \sigma_2 \end{pmatrix} |\xi\rangle\,, \quad \psi(x^3 = 0) \propto \begin{pmatrix} \mathbb{1}_2 - \sigma_3 \\ i(\mathbb{1}_2 + \sigma_3) \end{pmatrix} |\xi\rangle\,. \tag{4.89}$$

Since the operator $\mathbb{1}_2 \pm \sigma_3$ is a projector onto $\uparrow$ and $\downarrow$ spin state, we obtain the edge state $\psi(x^3 = 0)$ by applying $\downarrow$-spin projection to A sites, and $\uparrow$-spin projection to B sites at the $x^3 = 0$ plane. On the other hand, another edge state $\psi(x^2 = 0)$ is obtained by applying the spin rotation generated by σ_2 only to B site (nothing for A site) at the $x^2 = 0$ plane. The spectra of these boundary conditions are immediately obtained from (4.82) with the reduction

$$\epsilon_2(p) = \pm\sqrt{p_1^2 + p_3^2 + m^2}\,, \quad \epsilon_3(p) = \pm\sqrt{p_1^2 + p_2^2}\,, \tag{4.90}$$

and the gapless edge-of-edge spectrum (4.83). We now have the edge-of-edge state, but it seems difficult to detect its spectrum at this moment, because the spectrum $\epsilon_3(p)$ is also gapless in addition to the edge-of-edge state. In order to distinguish the edge-of-edge state from the edge states, we need to consider the situation such that only the edge-of-edge state is gapless, while the other edge states are gapped.

Before studying such a situation, let us discuss the reason why either of the edge spectra (4.90) is gapless, while the other is gapped. For the class AIII topological insulator, the

gapless edge state is protected by the chiral symmetry (4.86), which is indeed the sublattice symmetry. However, if the boundary condition is not compatible with the symmetry which protects the topological property, the edge state cannot be gapless any longer. This is essentially similar to the (class AII) topological insulator/ferromagnet junction [27]. The class AII topological insulator is protected by the time-reversal symmetry, but this symmetry can be weakly broken at the surface due to the junction with the ferromagnet. The role of ferromagnet can be replaced by the chiral superconductor, which breaks the time-reversal symmetry [28].

From this point of view, the edge state at $x^2 = 0$ shown in (4.89) breaks the sublattice symmetry because the σ_2-rotation acts only on the B-site, while the spin-projection applied to the edge state at $x^3 = 0$ could be consistent with the sublattice symmetry. Thus, to gap out the spectrum $\epsilon_3(p)$, we need to explicitly break the chiral (sublattice) symmetry for the edge state at $x^3 = 0$. For this purpose, we apply a rotated configuration

$$U_2 = \sigma_2 \cos\phi + i\mathbb{1}_2 \sin\phi\,,\ U_3 = i\mathbb{1}_2 \cos\phi - \sigma_3 \sin\phi\,, \tag{4.91}$$

which satisfies the compatibility condition (4.79). Then we obtain the gapped edge spectra

$$\epsilon_2(p) = \pm\sqrt{p_1^2 + p_3^2 + (m\cos\phi)^2}\,, \tag{4.92}$$

$$\epsilon_3(p) = \pm\sqrt{p_1^2 + p_2^2 + (m\sin\phi)^2}\,, \tag{4.93}$$

with the edge-of-edge state (4.83). Now only the edge-of-edge state is gapless, while the two edge states are gapped. This could be a suitable situation for experimental detection of the edge-of-edge state.

Chapter 5

Conclusion and discussions

5.1 Summary

In this thesis, I developed a methodology to study edge states in topological phases – boundary condition analysis. The basis procedure is as following: Starting from a model Lagrangian, by adding a generic surface term, we derive the equation of motion/Hamiltonian equation plus equation of boundary condition; by solving these equations we get edge states dispersion depending on momenta and boundary condition parameters.

I showed the validity and effectiveness of boundary condition analysis in three steps, the foundation, the development and the prediction, corresponding to three chapters in the thesis: Firstly, in the low energy limit, a simple Weyl fermion Hamiltonian is enough to characterize the topological structure of band-crossing points; secondly, the boundary condition analysis procedure gives explicit edge dispersions for three dimensional Weyl semimetals and its dimensional reduced case – topological insulator in two dimensions, in both continuum limit and on the lattice, covering the known results; thirdly, the boundary condition analysis gives prediction to a striking new exotic state – edge-of-edge state by its energy dispersion, in five dimensional Weyl semimetals and its dimensional reduced model – three dimensional topological insulator which can be realized in the experiments.

This thesis is a communication between particle physics and condensed matter physics. It is based on methodologies and techniques in either one or both of two subjects. On the level of methodology, I used topological facts of bands in condensed matter, lattice model relativistic dispersion of free fermions, dimensional reduction, etc. On the level of techniques, I intensively used algebras of gamma matrices and sigma matrices during the calculation of eigenvalue equations.

However, despite the similarities and things in common, in applying knowledges and experiences in particle theory to condensed matter physics, there are lots of gaps to fill in. Although both subjects uses relativistic quantum field theory, especially Dirac equation in cases of free fermions, the ways of using it are different. In condensed matter theory, the model Lagrangians are treated as effective description in which terms and coefficients can be modified depending on crystals, while in particle theory, there is only one model framework

determined by scattering experiments. During the study, I have realized that there are lots of practical issues to concern in writing down a appropriate Lagrangian/Hamiltonian for some bands.

With the validity of the Lagrangian, this thesis developed distinctive methodology: derive boundary condition by the surface term, giving rise to boundary dependent edge states. This also gives a message that unlike bulk states, edge states dispersion also depend on boundary parameters. With the benefit of the boundary condition parameter, bulk topological number and bulk-edge correspondence can be reinterpreted in our framework.

In this sense, as a student studying particle theory, I learned much from condensed matter physics.

5.2 Future direction

My previous researches of topological materials are based on topological numbers that can be defined by single particle wave function. This means the theory can only be applied to free fermions. In more generic situations when interactions are present, such kind of definition is not available. On the other hand, from particle physics theory we know that correlation functions in quantum field theories are related with observables — cross-section, for instance, and they are of vital importance. So can the correlation functions be used to define the topological number, how are the correlation functions are related with observables? These questions interest me very much and understanding them will be the near future goal of my research.

On the field theory side, there is a formula to compute topological number by free fermion propagator by K. Ishikawa and T. Matsuyama[29]. An advantage of the field theory approach is that it is possible to generalized to cases including electron-electron interactions. Field theory description, Chern-Simons effective theory approach by K. Ishikawa and T. Matsuyama is shown to be equivalent with Thouless-Kohmoto-Nightingale-den Nijss formalism for conductivity in integer quantum Hall effect[30] and possible to be generalized into interacting systems[31]. I want to investigate in this direction and see how topological numbers defined by fermion propagators can describe different topological phases.

Moreover correlation function/Green's function describes dynamical properties of excitations and has been a very successful method in most of areas in modern theoretical physics, such as scattering process in particle physics, phonon electron interaction in condensed matter physics, etc. Green's function gives many observables besides energy dispersion, such as thermodynamical quantities, density of states, etc. The systematic understanding of interacting topological phase phenomena requires a detailed study by applying Greens functions method. I want to understand the relation between correlation functions and all kinds of observables in topological materials.

Appendix A

A.1 Boundary conditions and Edge state at $x^a = 0$ $(a \neq 5)$

We look for a generic solution to the equation at the boundary

$$\psi_1^\dagger \Gamma^4 \psi_2 \Big|_{x^4=0} = 0 \tag{A.1}$$

which is analogous to (4.20). Its component expression is

$$\xi_1^\dagger \eta_2 + \eta_1^\dagger \xi_2 = 0\,. \tag{A.2}$$

A generic solution of this equation is obtained by a rotation in the 4-5 space from the previous one at $x^5 = 0$,

$$\psi = \begin{pmatrix} \mathbb{1}_2 - U_4 \\ \mathbb{1}_2 + U_4 \end{pmatrix} \chi(p_i, p_5) \exp[-\alpha_4 x^4] \tag{A.3}$$

with an arbitrary two-spinor η and a $U(2)$ matrix U_4. This U_4 parametrizes the boundary condition at $x^4 = 0$.

The boundary condition at $x^4 = 0$ can be written also as

$$\begin{pmatrix} \frac{1}{2}(U_4^\dagger - U_4) & \mathbb{1}_2 - \frac{1}{2}(U_4^\dagger + U_4) \\ \mathbb{1}_2 + \frac{1}{2}(U_4^\dagger + U_4) & -\frac{1}{2}(U_4^\dagger - U_4) \end{pmatrix} \psi \Big|_{x^4=0} = 0\,. \tag{A.4}$$

In this Appendix, we discuss the boundary conditions imposed to the 5d Weyl fermion (4.1) at the boundary $x^a = 0$ for $a = 1, 2, 3, 4$ in details. The boundary condition which we consider is

$$\psi^\dagger \Gamma^a \psi \Big|_{x^a=0} = 0 \quad (a = 1, 2, 3, 4)\,. \tag{A.5}$$

We use the notation of the Γ-matrices shown in (4.21). Applying the same argument discussed in Sec. 4.1, we obtain the corresponding localized edge state

$$\begin{aligned} (a = 1, 2, 3): \ \psi &= e^{-\alpha_a x^a} \begin{pmatrix} \mathbb{1}_2 + i\sigma_a U_a \\ i\sigma_a \left(\mathbb{1}_2 - i\sigma_a U_a\right) \end{pmatrix} \xi_a\,, \\ (a = 4): \ \psi &= e^{-\alpha_4 x^4} \begin{pmatrix} \mathbb{1}_2 - U_4 \\ \mathbb{1}_2 + U_4 \end{pmatrix} \xi_4\,, \end{aligned} \tag{A.6}$$

with $U_a \in U(2)$ and a two-spinor ξ_a. We remark that the boundary conditions (A.5) are rephrased as

$$\left(\mathbb{1}_2 + iU_a^\dagger\sigma_a \quad \left(\mathbb{1}_2 - iU_a^\dagger\sigma_a\right)(-i\sigma_a)\right)\psi\Big|_{x^a=0} = 0 \tag{A.7}$$

for $a = 1, 2, 3$, and

$$\left(\mathbb{1}_2 + U_4^\dagger \quad \mathbb{1}_2 - U_4^\dagger\right)\psi\Big|_{x^4=0} = 0 \tag{A.8}$$

for $a = 4$.

Let us then solve the spectrum of the edge state localized at $x^a = 0$. The eigen equation $\mathcal{H}\psi = \epsilon\psi$ for the Hamiltonian (4.1) with the boundary condition (A.5) for $a = 1$ leads to

$$\Big((i\alpha_1 - \epsilon) + (ip_5\sigma_1 - ip_2\sigma_2 - ip_3\sigma_3 + p_4)U_1\Big)\xi_1 = 0\,, \tag{A.9a}$$

$$\Big(-(i\alpha_1 + \epsilon)\,U_1 + (-ip_5\sigma_1 + ip_2\sigma_2 + ip_3\sigma_3 + p_4)\Big)\xi_1 = 0\,. \tag{A.9b}$$

We can similarly discuss the edge state localized at $x^2 = 0$, $x^3 = 0$, and also for $x^4 = 0$, which lead to the condition identical to that studied in Sec. 4.1 if we replace

$$(\alpha_a, p_5) \;\longrightarrow\; (\alpha_5, -p_a) \qquad (a = 1, 2, 3, 4)\,. \tag{A.10}$$

Thus we obtain

$$\epsilon_a(p) = p_4^{(a)}\cos\theta_a \pm \sqrt{|p_i^{(a)}|^2}\sin\theta_a\,, \tag{A.11}$$

$$\alpha_a(p) = -p_4^{(a)}\sin\theta_a \pm \sqrt{|p_i^{(a)}|^2}\cos\theta_a \tag{A.12}$$

where we decompose $U_a = e^{i\theta_a}U_a'$ with $U_a' \in SU(2)$, and define

$$(p_1^{(a)}, p_2^{(a)}, p_3^{(a)}, p_4^{(a)}) = \begin{cases} (-p_5, p_2, p_3, p_4) & (a = 1) \\ (p_1, -p_5, p_3, p_4) & (a = 2) \\ (p_1, p_2, -p_5, p_4) & (a = 3) \\ (p_1, p_2, p_3, -p_5) & (a = 4) \end{cases} \tag{A.13}$$

with the $SU(2)$-rotated momentum for $a = 1, 2, 3, 4$,

$$(-ip_i^{(a)}\sigma_i + p_4^{(a)})U_a' = -i\tilde{p}_i^{(a)}\sigma_i + \tilde{p}_4^{(a)}\,. \tag{A.14}$$

The normalization condition of the edge state is $\alpha_a > 0$.

A.2 Derivation of generic edge-of-edge dispersion relation

We show the derivation of the dispersion relation of generic edge-of-edge state localized at $x^4 = x^5 = 0$. Parametrizing the boundary condition matrices (4.61), the compatibility condition (4.59) becomes

$$\begin{aligned}&\det\big[\mathbb{1}_2 + B_0 - A_0 + A_\mu B^\mu + \\ &(B_i - A_i + A_i B_0 + A_0 B_i + i\epsilon_{ijk} A_j B_k)\sigma^i\big] = 0\,,\end{aligned} \tag{A.15}$$

which can be further written as:

$$\begin{aligned}&\mathbb{1}_2 + 2(B_0 - A_0) + A_0^2 - A_i^2 + B_0^2 - B_i^2 + 2A_0(B_0^2 - B_i^2) \\ &-2B_0(A_0^2 - A_i^2) + (A_0^2 - A_i^2)(B_0^2 - B_i^2) + 4A_i B_i = 0.\end{aligned} \tag{A.16}$$

Using the fact that $A_0^2 - A_i^2 = e^{2i\theta_5}$ and $B_0^2 - B_i^2 = e^{2i\theta_4}$, this is shown to be equivalent to

$$a_i b_i = -\cos\theta_4 \cos\theta_5 - i a_0 \sin\theta_4 + i b_0 \sin\theta_5\,, \tag{A.17}$$

and we arrive at the following two equations:

$$\begin{cases} a_i b_i = -\cos\theta_4 \cos\theta_5\,, & \text{(A.18)} \\ a_0 \sin\theta_4 = b_0 \sin\theta_5\,. & \text{(A.19)} \end{cases}$$

This is the generic constraint for the two boundary conditions, for the existence of the edge-of-edge states.

Next let us solve the energy eigen equations, (4.63) and (4.64). Denoting

$$p_5 := i\alpha_5 \tag{A.20}$$

and also

$$(i\sigma_j p_j + p_5)(b_0 + i b_i \sigma_i) = i\sigma_i \tilde{\tilde{p}}_i + \tilde{\tilde{p}}_5\,, \tag{A.21}$$

we have

$$\begin{cases} \tilde{\tilde{p}}_5 = b_0 p_5 - b_i p_i & \text{(A.22)} \\ \tilde{\tilde{p}}_i = b_0 p_i + b_i p_5 + \epsilon_{ijk} b_j p_k\,. & \text{(A.23)} \end{cases}$$

Then equations (4.63) and (4.64) become

$$\begin{cases} \epsilon\cos\theta_4 - \alpha_4 \sin\theta_4 + \tilde{\tilde{p}}_5 = 0\,, & \text{(A.24)} \\ (\epsilon\sin\theta_4 + \alpha_4\cos\theta_4)^2 - \tilde{\tilde{p}}_i^2 = 0\,. & \text{(A.25)} \end{cases}$$

These two equations are related by $\epsilon^2 = \tilde{\tilde{p}}_i^2 + \tilde{\tilde{p}}_5^2 - \alpha_4^2$, so instead, we shall use the following equivalent set of equations,

$$\begin{cases} \epsilon \cos\theta_4 - \alpha_4 \sin\theta_4 = b_i p_i - b_0 p_5 \,, & \text{(A.26)} \\ \epsilon^2 = p_i^2 - \alpha_4^2 - \alpha_5^2 & \text{(A.27)} \end{cases}$$

for convenience. Since (A.20) means that p_5 is pure imaginary, above two equations are actually three real equations including $b_0 p_5 = 0$, which means

$$b_0 = 0 \,, \tag{A.28}$$

and

$$\epsilon \cos\theta_4 - \alpha_4 \sin\theta_4 = b_i p_i. \tag{A.29}$$

Similarly, consider the boundary condition on the x^5 direction. Substitute equation (4.24) into the energy eigen equation and repeat the procedures starting from equations (4.63) and (4.64). Then we obtain

$$\begin{cases} \epsilon \cos\theta_5 - \alpha_5 \sin\theta_5 = a_i p_i \,, & \text{(A.30)} \\ a_0 = 0 \,. & \text{(A.31)} \end{cases}$$

Combining equations (A.29) (A.30) and (A.27) to eliminate α_4 and α_5, we obtain

$$A\epsilon^2 - 2B\epsilon + C = 0 \,, \tag{A.32}$$

which is (4.66) with the coefficients defined in (4.67).

References

[1] H. Weyl, "Elektron und Gravitation. I," *Zeitschrift für Physik*, vol. 56, pp. 330–352, May 1929.

[2] G. Backenstoss, "Helicity of μ^- minus Mesons from π-Meson Decay," *Physical Review Letters*, vol. 6, no. 8, pp. 415–416, 1961.

[3] S. Murakami, "Phase transition between the quantum spin hall and insulator phases in 3d: emergence of a topological gapless phase," *New Journal of Physics*, vol. 9, pp. 356–356, Sep 2007.

[4] X. Wan, "Topological semimetal and Fermi-arc surface states in the electronic structure of pyrochlore iridates," *Physical Review B*, vol. 83, no. 20, 2011.

[5] A. A. Burkov, "Weyl semimetal in a topological insulator multilayer," *Physical Review Letters*, vol. 107, no. 12, 2011.

[6] S.-M. Huang, S.-Y. Xu, I. Belopolski, C.-C. Lee, G. Chang, B. Wang, N. Alidoust, G. Bian, M. Neupane, C. Zhang, and et al., "A Weyl Fermion semimetal with surface Fermi arcs in the transition metal monopnictide TaAs class," *Nature Communications*, vol. 6, Jun 2015.

[7] S.-Y. Xu, I. Belopolski, N. Alidoust, M. Neupane, G. Bian, C. Zhang, R. Sankar, G. Chang, Z. Yuan, C.-C. Lee, and et al., "Discovery of a Weyl fermion semimetal and topological Fermi arcs," *Science*, vol. 349, pp. 613–617, Jul 2015.

[8] B. Lv, "Experimental Discovery of Weyl Semimetal TaAs," *Physical Review X*, vol. 5, no. 3, 2015.

[9] Z. K. Liu, L. X. Yang, Y. Sun, T. Zhang, H. Peng, H. F. Yang, C. Chen, Y. Zhang, Y. F. Guo, D. Prabhakaran, M. Schmidt, Z. Hussain, S.-K. Mo, C. Felser, B. Yan, and Y. L. Chen, "Evolution of the Fermi surface of Weyl semimetals in the transition metal pnictide family," *Nature Mat.*, vol. 15, pp. 27–31, nov 2015.

[10] H. Nielsen and M. Ninomiya, "Absence of neutrinos on a lattice: (i). proof by homotopy theory," *Nuclear Physics B*, vol. 185, no. 1, pp. 20 – 40, 1981.

[11] H. Nielsen and M. Ninomiya, "Absence of neutrinos on a lattice: (ii). intuitive topological proof," *Nuclear Physics B*, vol. 193, no. 1, pp. 173 – 194, 1981.

[12] D. B. Kaplan, "A method for simulating chiral fermions on the lattice," *Physics Letters B*, vol. 288, no. 3, pp. 342 – 347, 1992.

[13] M. F. Golterman, K. Jansen, and D. B. Kaplan, "Chern-Simons currents and chiral fermions on the lattice," *Physics Letters B*, vol. 301, no. 2, pp. 219 – 223, 1993.

[14] Y. Hatsugai, "Chern number and edge states in the integer quantum Hall effect," *Phys. Rev. Lett.*, vol. 71, no. 22, p. 3697, 1993.

[15] X.-G. Wen, *Quantum Field Theory of Many-Body Systems: From the Origin of Sound to an Origin of Light and Electrons*. Oxford Univ. Press, 2004.

[16] R. Jackiw and C. Rebbi, "Solitons with Fermion Number 1/2," *Phys. Rev.*, vol. D13, pp. 3398–3409, 1976.

[17] J. D. Jackson, *Classical Electrodynamics*. Wiley, 1998.

[18] L. Isaev, Y. H. Moon, and G. Ortiz, "Bulk-boundary correspondence in three-dimensional topological insulators," *Phys. Rev.*, vol. B84, p. 075444, 2011.

[19] V. V. Enaldiev, I. V. Zagorodnev, and V. A. Volkov, "Boundary Conditions and Surface States Spectra in Topological Insulators," *JETP Lett.*, vol. 101, pp. 89–96, 2015.

[20] H. Fukaya, T. Onogi, S. Yamamoto, and R. Yamamura, "Six-dimensional regularization of chiral gauge theories," *Progress of Theoretical and Experimental Physics*, vol. 2017, Mar 2017.

[21] K. Hashimoto and T. Kimura, "Topological Number of Edge States," *Phys. Rev.*, vol. B93, no. 19, p. 195166, 2016.

[22] E. Witten, "Three Lectures On Topological Phases of Matter," *La Rivista del Nuovo Cimento*, 2016.

[23] K. Hashimoto, T. Kimura, and X. Wu, "Boundary conditions of Weyl semimetals," *Progress of Theoretical and Experimental Physics*, vol. 2017, May 2017.

[24] K. Hashimoto, X. Wu, and T. Kimura, "Edge states at an intersection of edges of a topological material," *Physical Review B*, vol. 95, Apr 2017.

[25] W. A. Benalcazar, B. A. Bernevig, and T. L. Hughes, "Quantized Electric Multipole Insulators," *Science*, vol. 357, pp. 61–66, Jul 2017.

[26] S.-T. Wang, D.-L. Deng, and L.-M. Duan, "Probe of Three-Dimensional Chiral Topological Insulators in an Optical Lattice," *Phys. Rev. Lett.*, vol. 113, p. 033002, jul 2014.

[27] X.-L. Qi, T. Hughes, and S.-C. Zhang, "Topological Field Theory of Time-Reversal Invariant Insulators," *Phys. Rev.*, vol. B78, p. 195424, 2008.

[28] L. Fu and C. L. Kane, "Superconducting proximity effect and majorana fermions at the surface of a topological insulator," *Phys. Rev. Lett.*, vol. 100, no. 9, p. 096407, 2008.

[29] K. Ishikawa and T. Matsuyama, "A microscopic theory of the quantum Hall effect," *Nuclear Physics B*, vol. 280, pp. 523 – 548, 1987.

[30] D. J. Thouless, "Quantized Hall Conductance in a Two-Dimensional Periodic Potential," *Physical Review Letters*, vol. 49, no. 6, pp. 405–408, 1982.

[31] M. Zubkov, "Wigner transformation, momentum space topology, and anomalous transport," *Annals of Physics*, vol. 373, pp. 298 – 324, 2016.